JPET Fast Forward. Published on September 3, 2014 as DOI: 10.1124/jpet.114.218735
This article has not been copyedited and formatted. The final version may differ from this version.

JPET #218735

The pro-cognitive and synaptogenic effects of angiotensin IV-derived peptides are dependent on activation of the hepatocyte growth factor/c-Met system

Authors:

Caroline C. Benoist*, Leen H. Kawas*, Mingyan Zhu, Katherine A. Tyson, Lori Stillmaker, Suzanne M. Appleyard, John W. Wright, Gary A. Wayman, and, Joseph W. Harding

Affiliations:

Department of Integrative Physiology and Neuroscience, Washington State University, Pullman, WA, 99164-6520- JWH, CCB, LHK, JB, MZ, KAT, LS, SMA, GAW, JWW

Department of Psychology, Washington State University, Pullman, WA, 99164-4820- JWH, JWW

M3 Biotechnology, Inc. 4000 Mason Rd Suite 300, Box 352141, Seattle WA 98195-214- JWH, JWW, LHK

JPET Fast Forward. Published on September 3, 2014 as DOI: 10.1124/jpet.114.218735
This article has not been copyedited and formatted. The final version may differ from this version.

Running Title: Pro-cognitive/synaptogenic activity of HGF mimetics

Corresponding Authors:

Joseph W Harding
Department of Integrative Physiology and Neuroscience
Washington State University
Pullman, WA, 99164-6520
Email: hardingj@vetmed.wsu.edu

Gary A Wayman
Department of Integrative Physiology and Neuroscience
Washington State University
Pullman, WA, 99164-6520
Email: waymang@vetmed.wsu.edu

Number of Pages:

48

Number of Figures:

7

Number of Words:

- Abstract- 189
- Introduction- 547
- Discussion- 1408

Abbreviations:

AngIV: Angiotensin IV (VYIHPF)
IRAP: insulin-regulated membrane aminopeptidase
Nle-AngIV: Norleucine^{1}-AngIV
Dihexa: N-hexanoic-YI-(6) aminohexanoic amide
Hinge: KDYIRN
Norleucine-X-6 aminohexanoic family: D-Nle-X (an amino acid)-I-(6) aminohexanoic amide
Norleual: Nle-YL-Ψ(CH_2-NH_2)-HPF
im: intramuscular
aCSF: artificial cerebrospinal fluid
mRFP: monomeric red fluorescent protein
PIPES: piperazine-N,N′-bis(2-ethanesulfonic acid
HEPES: 4-(2-hydroxyethyl)-1-piperazineethanesulfonic acid
EGTA: ethylene glycol tetraacetic acid
TFP: tomato fluorescent protein
α-VGLUT1: Vesicular glutamate transporter 1
TTX: tetrodotoxin
mEPSC: miniature excitatory postsynaptic current
HGF: Hepatocyte growth factor
BS3: bissulfosuccinimidyl suberate

JPET Fast Forward. Published on September 3, 2014 as DOI: 10.1124/jpet.114.218735
This article has not been copyedited and formatted. The final version may differ from this version.

MDCK: Madin Darby canine kidney cells
HEK298: Human Embryonic Kidney 293 cell

ABSTRACT

A subset of angiotensin IV (AngIV)-related molecules are known to possess pro-cognitive/ anti-dementia properties and have been considered as templates for potential therapeutics. However, this potential has not been realized because of two factors: 1) a lack of blood-brain barrier (BBB) penetrant analogs; and 2) the absence of a validated mechanism of action. The pharmacokinetic barrier has recently been overcome with the synthesis of the orally active, BBB permeable analog Dihexa (N-hexanoic-tyrosine-isoleucine-(6) aminohexanoic amide) (McCoy *et al.*, 2013). Therefore, the goal of this study was to elucidate the mechanism that underlies Dihexa's pro-cognitive activity. Here we demonstrate that Dihexa binds with high affinity to hepatocyte growth factor (HGF) and both Dihexa and its parent compound Norleucine 1-AngIV (Nle^1-AngIV) induce c-Met phosphorylation in the presence of subthreshold concentrations of HGF and augment HGF-dependent cell scattering. Further, Dihexa and Nle^1-AngIV induce hippocampal spinogenesis and synaptogenesis similar to HGF itself. These actions were inhibited by an HGF antagonist and a sh-RNA directed at c-Met. Most importantly the pro-cognitive/anti-dementia capacity of orally delivered Dihexa was blocked by an HGF antagonist delivered intracerebroventricularly as measured using the Morris water maze task of spatial learning.

INTRODUCTION

While Angiotensin IV (AngIV; VYIHPF), and several AngIV analogs have long been known to possess marked pro-cognitive and anti-dementia activities (reviewed in Wright and Harding, 2013) questions have persisted regarding their mechanism of action and the identity of the molecular target mediating these effects. In 1992 our laboratory (Harding *et al.*) reported that a binding site, subsequently referred to as the angiotensin IV receptor subtype (AT_4; de Gasparo *et al.*, 1995) bound AngIV with high specificity and affinity. The identity of this protein has been a matter of continuing controversy. One possibility was first offered by Albiston and colleagues (2001) in the form of insulin-regulated membrane aminopeptidase (IRAP). These authors proposed that the physiological actions of AngIV-related ligands resulted from competitive inhibition of IRAP, thus potentiating the actions of endogenous neuropeptides normally degraded by IRAP. This model predicted that the action of all AngIV-related ligands should be qualitatively equivalent since their action is due to competitive interference with IRAP's peptidase activity. This notion is inconsistent with the existence of both agonists and antagonists, which exert opposite physiological actions (Wright *et al.*, 1999; Kramer *et al.*, 1997; Kramer *et al.*, 2001; Hamilton *et al.*, 2001). Further, this model predicts that the physiological effects of AngIV-related ligands should be slow to materialize since this action requires an accumulation of endogenous ligands. Again this prediction does not agree with the observation that AngIV-related ligands have rapid effects on signaling molecules (Chen *et al.*, 2001; Handa, 2001; Li *et al.*, 2002). Questions surrounding the functional linkage between AngIV-related ligands and IRAP were further amplified by a study that examined the cognitive capabilities of IRAP knockout mice (Albiston *et al.*, 2010). The results of this study indicated that contrary to

JPET Fast Forward. Published on September 3, 2014 as DOI: 10.1124/jpet.114.218735
This article has not been copyedited and formatted. The final version may differ from this version.

the "AngIV/IRAP: inhibition of endogenous peptide metabolism" hypothesis spatial learning was modestly impaired rather than facilitated as predicted.

If the interaction of AngIV-related peptides with IRAP is not responsible for the profound biological activities of these molecules, then what is the mechanism? Initial hints of a possible target are apparent in several studies that examined the mechanism of action of "AT_4 receptor antagonists" (Kawas *et al.*, 2011; Kawas *et al.*, 2012; Yamamoto *et al.*, 2010), which were originally defined as AngIV-like molecules that interfered with cognition (Wright *et al.*, 1999). These studies demonstrated that the antagonists had structural homology with the dimerization domain of the pleiotropic growth factor hepatocyte growth factor (HGF), bound to HGF with high affinity, blocked HGF's activation and subsequent activation of its receptor c-Met, and displayed both anti-cancer and anti-angiogenic activity as would be expected of an HGF/c-Met antagonist (Peters and Adjei, 2012). While these results clearly linked the action of "AT_4 receptor antagonists" to the HGF/c-Met system they did not provide a suitable explanation for the mechanism underlying the pro-cognitive activity of "AT_4 receptor agonists".

Thus the goal of the present study was to provide that explanation. Nle^1-AngIV, an often employed "AT_4 receptor agonist", with demonstrated pro-cognitive activity (Benoist *et al.*, 2011) along with its metabolically stabilized and orally active derivative, Dihexa (McCoy *et al.*, 2013) were utilized to probe this question. Both agonists were found to potentiate the cellular actions of HGF. Results indicate that it is this ability to activate HGF that is responsible for both the marked synaptogenic and pro-cognitive activities of these compounds.

JPET Fast Forward. Published on September 3, 2014 as DOI: 10.1124/jpet.114.218735
This article has not been copyedited and formatted. The final version may differ from this version.

MATERIALS AND METHODS

Compounds and Peptide Synthesis:

Scopolamine hydrobromide (#S-1875) was purchased from Sigma Chemical (St Louis, MO). The peptides were synthesized using Fmoc-based solid-phase peptide synthesis methods and purified by reverse phase HPLC in the Harding laboratory. Purity and structure were verified by LC-MS. Hepatocyte growth factor (HGF) was purchased from R&D Systems (Minneapolis, MN). ^{3}H- Dihexa (N-hexanoic-tyrosine-isoleucine-(6) aminohexanoic amide [tyrosine-2, 6-^{3}H) with a specific activity = 33.5 Ci/mmol and an HPLC purity >99% was custom synthesized by ViTrax (Placentia, CA).

Animals and Surgery:

Male Sprague-Dawley rats (Taconic derived) weighing 390-450 g were maintained with free access to water and food (Harland Tekland F6 rodent diet, Madison, WI), except the night prior to surgery when food was removed. Each animal was anesthetized with Ketamine hydrochloride plus Xylazine (100 and 2 mg/kg *im* respectively; Phoenix Scientific; St. Joseph, MO, and Moby; Shawnee, KS). An intracerebroventricular (*icv*) guide cannula (PE-60, Clay Adams; Parsippany, NY) was stereotaxically positioned (Model 900, David Kopf Instruments; Tujunga, CA) in the right hemisphere using flat skull coordinates 1.0 mm posterior and 1.5 mm lateral to bregma (refer to Wright *et al.*, 1985). The guide cannula measured 2.5 cm in overall length and was prepared with a heat bulge placed 2.5 mm from its beveled tip, thus acting as a stop to control the depth of penetration. Once in position, the cannula was secured to the skull with two stainless-steel screws and dental cement. Post-operatively the animals were housed individually in an American Accreditation for Laboratory Animal Care-approved vivarium maintained at 22 ± 1°C

JPET Fast Forward. Published on September 3, 2014 as DOI: 10.1124/jpet.114.218735
This article has not been copyedited and formatted. The final version may differ from this version.

on a 12-h alternating light/dark cycle initiated at 06:00 h. All animals were hand gentled for 5 days.

Behavioral Testing:

The water maze consisted of a circular tank painted black (diameter: 1.6 m; height: 0.6 m), filled to a depth of 26 cm with 26-28°C water. A black circular platform (diameter: 12 cm; height: 24 cm) was placed 30 cm from the wall and submerged 2 cm below the water surface.

The maze was operationally sectioned into four equal quadrants designated NW, NE, SW, and SE. For each rat the location of the platform was randomly assigned to one of the quadrants and remained fixed throughout the duration of training. Entry points were at the quadrant corners (i.e., N, S, E, and W) and were pseudo-randomly assigned such that each trial began at a different entry point than the preceding trial. Three of the four testing room walls were covered with extra-maze spatial cues consisting of different shapes (circles, squares, triangles) and colors. The swimming path of the animals was recorded using a computerized video tracking system (Chromotrack; San Diego Instruments, CA). The computer displayed only total swim latency.

Each member of the treatment groups received an *icv* injection of scopolamine hydrobromide (70 nmol in 2 µl aCSF over a duration of 20 s) or aCSF (control) 20 min prior to testing followed by oral Dihexa (2 mg/kg/day) or saline (control). When employed, Hinge (KDYIRN; 300 pmol in 2 µl aCSF), or aCSF (control) was delivered by icv injection 5 min prior to testing. The behavioral testing protocol has been described previously in detail (Wright *et al.*, 1999). Briefly, acquisition trials were conducted on 8 consecutive days with 5 trials/day. On the first day of training the animal was placed on the pedestal for 30 s prior to the first trial. Trials commenced with the placement of the rat facing the wall of the maze at one of the assigned entry points. The rat was allowed a maximum of 120 s to locate the platform. Once the animal located the

JPET Fast Forward. Published on September 3, 2014 as DOI: 10.1124/jpet.114.218735
This article has not been copyedited and formatted. The final version may differ from this version.

platform it was permitted a 30-s rest period on the platform. If the rat did not find the platform, the experimenter placed the animal on the platform for the 30-s rest period. The next trial commenced immediately following the rest period. Upon completion of each daily set of trials the animal was towel-dried and placed under a 100 watt lamp for 10-15 min and then returned to its home cage.

Dendritic Spine Analysis:

Hippocampal Cell Culture Preparation. Hippocampal neurons (2×10^5 cells per square cm) were cultured from P1 Sprague Dawley rats on plates coated with poly-L-lysine from Sigma (St. Louis, MO; molecular weight ~300,000). Hippocampal neurons were maintained in Neurobasal A media from Invitrogen (Carlsbad, CA) supplemented with B27 from Invitrogen, 0.5 mM L-glutamine, and 5 mM cytosine-D-arabinofuranoside from Sigma added on the second day in culture. Hippocampal neurons were then cultured a further 3-7 days, at which time they were either transfected or treated with various pharmacological reagents as described in (Wayman *et al.*, 2008).

Transfection. Neurons were transfected with mRFP-β-actin on day *in vitro* 6 (DIV6) using LipofectAMINE 2000 (Invitrogen) according to the manufacturer's protocol. This protocol yielded the desired 3-5% transfection efficiency thus enabling the visualization of individual neurons. Higher efficiencies obscured the dendritic arbor of individual neurons. Expression of fluorescently tagged actin allowed clear visualization of dendritic spines, as dendritic spines are enriched in actin. On DIV7 the cells were treated with vehicle (H_2O) or peptides (as described in the text) added to media. On DIV12 the neurons were fixed (4% paraformaldehyde, 3% sucrose, 60 mM PIPES, 25 mM HEPES, 5 mM EGTA, 1 mM $MgCl_2$, pH 7.4) for 20 min at room temperature and mounted.

JPET Fast Forward. Published on September 3, 2014 as DOI: 10.1124/jpet.114.218735
This article has not been copyedited and formatted. The final version may differ from this version.

Slides were dried for at least 20 h at 4°C and fluorescent images were obtained with Slidebook 4.2 Digital Microscopy Software driving an Olympus IX81 inverted confocal microscope with a 60X oil immersion lens, NA 1.4 and resolution 0.280 µm. Dendritic spine density was measured on primary and secondary dendrites at a distance of at least 150 µm from the soma. Five 50 µm long segments of dendrites from at least 10 neurons were analyzed for each data point reported. Each experiment was repeated at least three times using independent culture preparations. Spines were manually counted. Spines were considered dendritic protrusions with an actin rich head, which had a diameter 1.5 times that of the protrusion shaft.

Organotypic Hippocampal Slice Culture Preparation and Transfection. Hippocampi from P4 Sprague Dawley rats were cultured as previously described (Wayman *et al.*, 2006). In order to visualize dendritic arbors 400 µm hippocampal slices from postnatal day 5 were cultured for 3 days after which they were biolistically transfected with tomato fluorescent protein (TFP) using a Helios Gen Gun (Bio-Rad; Hercules, CA), according to the manufacturer's protocol. Following a 24-h recovery period slices were stimulated with vehicle (H_2O), 1 pM Nle^1-AngIV or Dihexa for 2 days. Slices were fixed and mounted. Hippocampal CA1 neuronal processes were imaged and measured as described above.

Immunocytochemistry. Transfected neurons were treated and fixed as described above. Following fixation, cells were permeabilized with 0.1% Triton X-100 detergent (Bio-Rad; Hercules, CA), blocked with 8% bovine serum albumin (Intergen Company; Burlington, MA) in PBS followed by an incubation period with anti- α-VGLUT1 (Synaptic Systems; Goettingen, Germany), anti-synapsin (Synaptic Systems; Goettingen, Germany), anti-PSD-95 (Millipore; Billerica, MA) following the manufacturers protocol, at 4°C. Subsequently cells were rinsed twice with PBS, incubated in Alexafluor 488 goat-anti-mouse following the manufacturer's

JPET Fast Forward. Published on September 3, 2014 as DOI: 10.1124/jpet.114.218735
This article has not been copyedited and formatted. The final version may differ from this version.

protocol (Invitrogen: Carlsbad, CA) for 2 h at room temperature, rinsed again with PBS, and mounted with ProLong Gold anti-fade reagent (Invitrogen; Carlsbad, CA). Imaging and analysis were performed as described above.

Whole-Cell Recordings. Patch-clamp experiments were performed on mRFP-β-actin transfected cultured hippocampal neurons with PBS (vehicle control) or 1 pM Nle^1-AngIV pretreatment. Recordings were made on DIV12-14. The culture medium was exchanged by an extracellular solution containing (in mM) 140 NaCl, 2.5 KCl, 1 $MgCl_2$, 3 $CaCl_2$, 25 glucose, and 5 HEPES; pH was adjusted to 7.3 with KOH; and osmolality was adjusted to 306-310 mOsm. Cultures were allowed to equilibrate in a recording chamber mounted on inverted microscope (IX-71; Olympus optical, Tokyo) for 30 min before recording. Transfected cells were visualized with fluorescence (Olympus Optical). Recording pipettes were pulled (P-97 Flaming/Brown micropipette puller; Sutter Instrument; Novato, CA) from standard-wall borosilicate glass without filament (OD = 1.5 mm; Sutter Instrument). The resistance of patch electrodes ranged from 4.0 to 5.2 MΩ, and were filled with an internal solution of the following composition (in mM): 25 CsCl, 100 $CsCH_3O_3S$, 10 phosphocreatine, 0.4 EGTA, 10 HEPES, 2 $MgCl_2$, 0.4 Mg-ATP, and 0.04 Na-GTP; pH was adjusted to 7.2 with CsOH; osmolality was adjusted to 298-300 mOsm. Miniature EPSCs (mEPSCs) were isolated pharmacologically by blocking $GABA_A$ receptor channels with picrotoxin (100 μM; Sigma), glycine receptors with strychnine (1 μM; Sigma), and sodium channels with tetrodotoxin (TTX, 500 nM; R&D Systems; Minneapolis, MN). Recordings were obtained using a Multiclamp 700B amplifier (Molecular Devices; Sunnyvale, CA). Analog signals were low-pass Bessel filtered at 2 kHz, digitized at 10 kHz through a Digidata 1440A interface (Molecular Devices), and stored in a computer using Clampex 10.2 software (Molecular Devices). The membrane potential was held at -70 mV at

JPET Fast Forward. Published on September 3, 2014 as DOI: 10.1124/jpet.114.218735
This article has not been copyedited and formatted. The final version may differ from this version.

room temperature (25°C) during a period of 0.5-2 h after removal of the culture from the incubator. Liquid junction potentials were not corrected. Data analysis was performed using Clampfit 10.2 software (Molecular Devices), and Mini-Analysis 6.0 software (Synaptosoft Inc.; Fort Lee, NJ). The criteria for a successful recording included an electrical resistance of the seal between the outside surface of the recording pipette and the attached cell >2 GΩ and a neuron input resistance >240 MΩ. The mEPSCs had a 5-min recording time.

HGF Binding:

The binding of ^{3}H-Dihexa to HGF was assessed using a soluble binding assay. Saturation isotherms were developed for the interaction of ^{3}H-Dihexa with HGF. 250µl of PBS containing human HGF (1.25 ng) were incubated with multiple concentrations of ^{3}H-Dihexa ranging from 10^{-13} M to 10^{-8} for 40 min at 37°C. Preliminary kinetic studies indicated that equilibrium binding was reached by 40 min of incubation at 37°C. The incubates were then spun through Bio-Gel P6 spin columns (400 µl packed volume) for 1 min to separate free and bound ^{3}H-Dihexa and the eluent collected. Five milliliters of scintillation fluid was added to the eluent, which contained the HGF bound ^{3}H-Dihexa, and then counted using a scintillation counter. Total disintegrations per minute of bound ^{3}H-Dihexa were calculated based on machine counting efficiency. Saturation isotherms were performed in quadruplicate. The affinity of ^{3}H-Dihexa for HGF (Kd) and total binding (Bmax) were determined, using the Prism 5 and InStat v.3.05 graphical/statistical programs (GraphPad, San Diego).

Dimerization:

HGF dimerization was assessed using PAGE followed by silver staining. Human HGF, at a concentration of 0.08 ng/µl with or without drugs, was incubated with heparin at a final concentration of 5 µg/ml. 25 mM BS3 cross-linker (Pierce Chemical; Rockford, IL) was then

JPET Fast Forward. Published on September 3, 2014 as DOI: 10.1124/jpet.114.218735
This article has not been copyedited and formatted. The final version may differ from this version.

added to the reaction for 30 min at 37°C. Subsequently the reaction was quenched with 20 mM Tris buffer. Qualitatively identical results were also obtained in the absence of BS3 attesting to the high affinity of the HGF/HGF dimer. Loading buffer was then added to each sample and the mixture separated by native PAGE using gradient Criterion XT precast gels (4-12% Bis-Tris; Bio-Rad Laboratories; Hercules, CA). Similar results were obtained in the presence of SDS. Next the gel was silver stained for the detection of the HGF monomers and dimers. Bands were quantitated from digital images using a UVP phosphoimager (Upland, CA).

Western Blotting:

HEK293 cells were seeded in 6-well tissue culture plates and grown to 95% confluency in DMEM containing 10% FBS. The cells were serum deprived for 24 h prior to the treatment to reduce the basal levels of phospho-Met. Following serum starvation, cocktails comprised of vehicle and HGF with/without Dihexa or Nle^1-AngIV were prepared and pre-incubated for 30 min at room temperature. The cocktail was then added to the cells for 10 min to stimulate the Met receptor activation. Cells were harvested using RIPA lysis buffer (Upstate) supplemented with phosphatase inhibitor cocktails 1 and 2 (Sigma-Aldrich; St. Louis, MO). The lysate was clarified by centrifugation at 15,000 g for 15 min, protein concentrations were determined using the BCA total protein assay, and then appropriate volumes of the lysates were diluted with 2X reducing Laemmli buffer and heated for ten minutes at 95°C. Samples containing identical amounts of protein were resolved using SDS-PAGE (Criterion; Bio-Rad Laboratories), transferred to nitrocellulose, and blocked in Tris-buffered saline (TBS) containing 5% milk for 1 h at room temperature. The phospho-Met antibody or total Met antibody, were added to the blocking buffer at a final concentration of 1:1000 and incubated at 4°C overnight with gentle agitation. The membranes were then washed several times with water and TBS (PBS, 0.05%

Tween-20), a 1:5000 dilution of horseradish-peroxidase conjugated goat anti-rabbit antiserum was added, and the membranes further incubated for 1 h at room temperature. Proteins were visualized using the Supersignal West Pico Chemiluminescent Substrate system (Pierce; Fenton, MO) and molecular weights determined by comparison to protein ladders (BenchMark, Invitrogen; and Kaleidoscope, Bio-Rad). Images were digitized and analyzed using a UVP phosphoimager.

shRNA:

A target sequence for c-Met was designed using RNAi central design program (http://cancan.cshl.edu/). The target sequence GTGTCAGGAGGTGTTTGGAAAG was inserted into pSUPER vector (Oligoengine; Seattle WA) which drives endogenous production of shRNA under the H1 promoter. The shRNA was transfected into cells using the lipofectamine method described above. Verification of receptor knockdown was done by creating a c-Met-6-Myc tagged gene product using the Gateway cloning system (Invitrogen). The Met protein coding sequence was cloned from rat whole brain cDNA using primers obtained from Integrated DNA Technologies, Inc. The amplified product was gel purified and a band corresponding to 190 kDa band excised and cloned into a pCAGGS-6-Myc destination vector (Gateway).

Scattering Assay:

MDCK cells were grown to 100% confluency on the coverslips in 6-well plates and washed twice with PBS. The confluent coverslips were then aseptically transferred to new 6-well plates containing 900 µl serum free DMEM. Nle^1-AngIV, Dihexa, and/or HGF (20 ng/ml) were added to appropriate wells. Control wells received PBS vehicle. Plates were incubated at 37°C with 5% CO_2 for 48 h. Media was removed and cells were fixed with methanol. Cells were stained with Diff-Quik Wright-Giemsa (Dade-Behring; Newark, DE) and digital images were taken.

JPET Fast Forward. Published on September 3, 2014 as DOI: 10.1124/jpet.114.218735
This article has not been copyedited and formatted. The final version may differ from this version.

Coverslips were removed with forceps and more digital images were captured. Pixel quantification of images was achieved using Image J and statistics were performed using Prism 5 and InStat v.3.05.

Statistical Analyses:

The Morris water maze data sets, consisting of mean latencies and path distances to find the platform during each daily block of five trials, were calculated for each animal for each day of acquisition. Overall differences in learning curves were assessed with two-way ANOVAs with repeated measures with Bonferoni correction. Additionally one-way ANOVAs were used to compare group latencies swum on various days of training. Significant effects were further analyzed by a Newman-Keuls post-hoc test with a level of significance set at $p < 0.05$.

One-way ANOVA was also used to analyze the dendritic spine and electrophysiology results and significant effects were analyzed by Tukey post-hoc test, with a level of significance set at $p < 0.05$. Numerical data are expressed as mean ± SEM.

RESULTS

- ***The AngIV Analog Binds to HGF with High Affinity and Inhibits HGF Dimerization.***

JPET Fast Forward. Published on September 3, 2014 as DOI: 10.1124/jpet.114.218735
This article has not been copyedited and formatted. The final version may differ from this version.

Previous studies from our laboratory have demonstrated that various AngIV analogs, which act as "AT_4 receptor antagonists" possess structural homology with the dimerization domain of HGF. These analogs bind HGF with high affinity while blocking HGF dimerization and ultimately its capacity to activate c-Met (Kawas *et al.*, 2011; 2012). Furthermore, there appears to be direct correlation between biological activity and the ability to inhibit HGF dimerization (Kawas *et al.*, 2012). While it was easy to envision how an antagonist could exert its effects by blocking the dimerization of HGF, a process linked to its activation (Gherardi *et al.*, 2006, Youles *et al.*, 2008), the same could not be said for structurally similar agonists, especially if they also engaged an HGF -dependent mechanism.

To begin to address this quandary (tyrosine-2, 6-^{3}H)-Dihexa was synthesized and its direct binding to HGF assessed. ^{3}H- Dihexa was found to bind HGF saturably and with high affinity (Kd = 65 pM) (Figure 1A). The ability of Dihexa to bind HGF raised the question as to its impact on the dimerization process. To address this question, native gels in combination with silver staining and densitometry were employed to visualize HGF monomers and multimers and quantitate the effect of Dihexa, and several representative antagonists on the dimerization process (Figure 1 B and C). Somewhat surprisingly Dihexa effectively inhibited HGF dimerization at 10^{-10} M concentration similar to that seem with HGF antagonists Norleual, Hinge, and Norleucine-X-6-aminohexanoic amide family analogs.. Although not directly addressed in these studies these data suggest that Dihexa and its parent compound Nle^{1}-AngIV might act allosterically to stabilize an active HGF conformation. Consistent with this hypothesis, we have recently demonstrated that c-Met is pre-multimerized on the dendrites of hippocampal neurons as dimers, tetramers, hexamers, and octomers in the absence of HGF; suggesting that the

JPET Fast Forward. Published on September 3, 2014 as DOI: 10.1124/jpet.114.218735
This article has not been copyedited and formatted. The final version may differ from this version.

HGF dimerization process likely subserves a function other than initiating receptor dimerization (Kawas *et al.*, 2013).

- ***Dihexa and Nle^1-AngIV Act Synergistically with HGF to Augment c-Met Signaling and HGF-dependent Cellular Activity.***

The notion that Dihexa and Nle^1-AngIV allosterically activate HGF predicts that these analogs should potentiate HGF's ability to activate its receptor and subsequent cellular responses. To evaluate this idea HEK-293 cells, which express c-Met, were stimulated with threshold levels of HGF in the presence of Dihexa and Nle^1-AngIV and the impact on c-Met activation (phosphorylation) was accessed (Figure 2A-D). . While Dihexa at 10^{-10} M and 10^{-12} M alone did not activate c-Met, Dihexa at both concentrations markedly augmented the capacity of HGF at 1.25 ng/ml and 2.5 ng/ml to activate c-Met (Figure 2A and B). . Similarly these concentrations of Nle^1-AngIV potentiated the ability of 1.25ng/ml and 2.5 ng/ml of HGF to activate c-Met (Figure 2C and D). However unlike Dihexa, Nle^1-AngIV alone at concentrations of 10^{-10} M and 10^{-12} M was capable of activating c-Met, perhaps suggesting an even higher affinity for HGF than Dihexa.

c-Met activation initiates multiple cellular responses including increased proliferation/survival, motility, and differentiation (Zhang and Vande Woude, 2003). Together, these cellular responses contribute to c-Met's hallmark effect of scattering, a process characterized by decreased cell adhesion, and increased motility and proliferation. In order to explore the physiological significance of Dihexa's and Nle^1-AngIV's ability to augment c-Met signaling, we evaluated the effect of Dihexa and Nle^1-AngIV on classic c-Met-dependent changes in cell behavior using Madin-Darby canine kidney (MDCK) cells, a standard cellular model for investigating the HGF/c-Met system (Stella and Comoglio, 1999). Stimulation with

JPET Fast Forward. Published on September 3, 2014 as DOI: 10.1124/jpet.114.218735
This article has not been copyedited and formatted. The final version may differ from this version.

Dihexa at 10^{-10} M facilitated HGF-dependent scattering while concentrations of 10^{-12} M and 10^{-14} M produced a dose-dependent trend toward potentiation that did not reach statistical significance (Figure 3A and B). Further, in the absence of exogenously applied HGF Dihexa at 10^{-12} M markedly augmented scattering suggesting the presence of endogenous HGF in the preparation. Consistent with the presence of endogenous HGF in the cultures Nle^1-AngIV at 10^{-8} M, 10^{-10} M, and 10^{-12} M supported cell scattering in the absence of added exogenous HGF (Figure 3C and D). Taken together these data indicate that both Dihexa and Nle^1-AngIV at subnanomolar concentrations are capable of potentiating the impact of HGF on both c-Met activation and subsequent cellular responses.

- ***Hepatocyte Growth Factor Augments the Dendritic Architecture and Supports Increased Spinogenesis.***

The ability of Dihexa and Nle^1-AngIV to stimulate hippocampal spinogenesis and synaptogenesis (McCoy *et al,* 2013) and their capacity to facilitate the actions of HGF predicts that HGF itself should enhance spinogenesis and synaptogenesis. As such, the effects of HGF on spinogenesis in dissociated hippocampal cultures were evaluated. To this end hippocampal neurons were transfected with mRFP-β-actin on day *in vitro* (DIV) 6, stimulated with HGF for 5 days, and subsequently analyzed for the number of dendritic spines.

A dose-dependent increase in spine numbers following HGF stimulation was observed with a lowest effective dose of 5 ng/ml (mean spine numbers = 24.7; **= $p < 0.01$ vs. control; ns vs. HGF 10 and 20 ng/ml). The most significant effects were produced by 10 and 20 ng/ml doses (mean spine numbers = 27.5 and 27.0 respectively; n = 50 per treatment group; *** = $p < 0.001$; df = 4/245; F = 13.5). However, the 2.5 ng/ml dose of HGF had no effect on basal spine

JPET Fast Forward. Published on September 3, 2014 as DOI: 10.1124/jpet.114.218735
This article has not been copyedited and formatted. The final version may differ from this version.

numbers (mean spine numbers = 18.6 vs. control = 18.0) (Figure 4A) and was therefore considered to be sub-threshold.

To further confirm the ability of HGF to augment spinogenesis in a more anatomically intact environment HGF-dependent spinogenesis in organotypic hippocampal slices was examined and compared to Dihexa. Hippocampal slices were biolistically transfected with the soluble red fluorescent protein Tomato and stimulated with 10 ng/ml HGF, 10^{-12} M Dihexa or vehicle for 48 h. CA1 hippocampal neurons, which are known to undergo plastic changes in response to learning and can be easily identified based on their location and morphologically characteristics, were evaluated for changes in spine numbers. Both Dihexa and HGF significantly increased the number of spines per 50 μm dendrite length in the CA1 hippocampal neurons (mean spine numbers = 15.0 and 18.5 respectively compared to mean control spine numbers = 6.1; *** = $P < 0.001$ and ** = $P < 0.01$ between treatment groups; df = 2/81; F = 41.5) (Figure 4B and C).

- ***Dihexa and Nle^1-AngIV Act Synergistically with HGF to Increase Hippocampal Neuron Spinogenesis.***

The capacity of Dihexa and Nle^1-AngIV to shift the HGF dose-response curve to the left in HEK293 cells coupled with their ability to augment spinogenesis in hippocampal neurons further anticipated that Dihexa and Nle^1-AngIV should similarly potentiate the spinogenic activity of HGF. To test this notion the combined effects of sub-threshold doses of HGF augmented with Dihexa or Nle^1-AngIV were evaluated as to their spinogenic activity in dissociated rat hippocampal neurons. Dissociated hippocampal neurons transfected with mRFP-β-actin were stimulated for 5 days with sub-threshold concentrations of HGF and Dihexa or Nle^1-AngIV (2.5 ng/ml + 10^{-13} M, respectively). Additionally, biologically active doses of HGF (10 ng/ml),

JPET Fast Forward. Published on September 3, 2014 as DOI: 10.1124/jpet.114.218735
This article has not been copyedited and formatted. The final version may differ from this version.

Dihexa or Nle^{1}-AngIV (10^{-12} M) or a combination of sub-threshold doses of 2.5 ng/ml HGF + 10^{-13} M Dihexa or 2.5 ng/ml HGF + 10^{-13} M Nle^{1}-AngIV were applied.

As expected, putative sub-threshold concentrations of HGF (2.5 ng/ml), Dihexa and Nle^{1}-AngIV (10^{-13} M) failed to alter basal spinogenesis and did not differ from control treated neurons (mean ± S.E.M. spine numbers for control = 17.4, HGF = 16.5, Dihexa = 17.1 and Nle^{1}-AngIV = 16.5 per 50 μm dendrite length; $p > 0.05$). In contrast, biologically active doses of HGF (10 ng/ml), Dihexa and Nle^{1}-AngIV (10^{-12} M) produced a significant effect over control treated spines (mean ± S.E.M. spine numbers for HGF = 29.3, Dihexa = 26.4 and Nle^{1}-AngIV = 29.8 per 50 μm dendrite). Combined sub-threshold doses of 2.5 ng/ml HGF + 10^{-13} M Dihexa and 2.5 ng/ml HGF + 10^{-13} M Nle^{1}-AngIV phenocopied the effects of each agonist at its biologically active dose alone (mean ± S.E.M. spine numbers for HGF + Dihexa are 28.8 and HGF + Nle^{1}-AngIV are 26.2 per 50 μm dendrite length compared to control treated neurons = 17.4; *** = $P < 0.001$; mean ± S.E.M.; by one-way ANOVA followed by Tukey post hoc test). Together these data (Figure 4D and E) further confirm that HGF and the HGF activators, Dihexa and Nle^{1}-AngIV act synergistically resulting in significant changes in neuronal structure.

- ***Dihexa, Nle^{1}-AngIV, and HGF Support the Development of Functional Synapses.***

Previous studies in which neurons were treated with Dihexa and Nle^{1}-AngIV indicated that most of the induced dendritic spines were co-localized with both pre- and postsynaptic markers indicative of functional synapses (Benoist *et al.*, 2011; McCoy *et al.*, 2013). Additionally the majority of synaptic input appeared to be glutamatergic. Because Dihexa and Nle^{1}-AngIV are suggested to operate via an HGF-dependent mechanism, the functional properties of HGF-induced spines were evaluated. mRFP-β-actin transfected hippocampal neurons were immunostained for a general marker of presynaptic active zones, synapsin (Ferreira and

JPET Fast Forward. Published on September 3, 2014 as DOI: 10.1124/jpet.114.218735
This article has not been copyedited and formatted. The final version may differ from this version.

Rapoport; 2002) as well as a marker specific for glutamatergic synapses, Vesicular Glutamate Transporter 1 (VGLUT1) (Balschun *et al.,* 2010). HGF stimulation significantly augmented the number of postsynaptic spines (Figure 4A). The number of postsynaptic spines (red) adjacent to VGLUT1, or synapsin-positive puncta (green) were counted and converted to a percentage of the total spines counted. For HGF-treated neurons (10 ng/ml) immunostained with anti-synapsin1, 98% of the actin-enriched spines co-distributed with synapsin1 (Figure 5A and B). Similarly 95% of the spines co-distributed with VGLUT1 indicating that spines induced by HGF were almost exclusively glutamatergic (Figure 5A and C). The co-distribution of green puncta representative of synapsin1 and VGTUT1 and mRFP-β-actin labeled spines for vehicle treated neurons exhibited a parallel 94% correlation (Figure 5A and B). The above data suggest that spines produced in response to HGF-treatment form functional synapses. Furthermore, the high correlation with VGLUT1 suggests that many of these inputs are excitatory in nature.

To further validate the conclusion that new spines supported functional synapses we measured the frequency of spontaneous AMPA receptor-mediated mini-excitatory postsynaptic currents (mEPSCs) from neurons following HGF treatment and compared these data to those obtained for Dihexa, which had been previously established to increase the number of morphologically identified synapses with a concomitant rise in the frequency of mEPSCs (McCoy *et al.,* 2013). Recordings were made in dissociated hippocampal neurons transfected with mRFP-β-actin and treated with 10^{-12} M Dihexa, 10 ng/ml HGF, or an equivalent volume of vehicle following 5 days of drug exposure. Both HGF (mean frequency = 5.84 ± 0.68; n = 9) and Dihexa treatment (mean frequency = 5.32 ± 1.01; n = 9) increased mEPSC frequency approximately two-fold over control treated neurons (mean frequency = 2.19 ± 0.75; n = 9; *** = $P < 0.012$ (HGF), and $P < 0.04$ (Dihexa); mean ± S.E.M. by one-way ANOVA followed by

JPET Fast Forward. Published on September 3, 2014 as DOI: 10.1124/jpet.114.218735
This article has not been copyedited and formatted. The final version may differ from this version.

Tukey post hoc test) (Figure 5E), supporting the supposition that HGF treatment increases synaptogenesis.

- ***The HGF Antagonist, Hinge, and a c-Met Specific sh-RNA Block the Biological Actions of HGF, Dihexa, and Nle^{1}-AngIV.***

Seeking further substantiation that the actions of Dihexa and Nle^{1}-AngIV are mediated through the HGF/c-Met system, the novel HGF antagonist Hinge (KDYIRN), and a shRNA targeting c-Met were employed to block the spinogenic and synaptogenic effects of Dihexa and Nle^{1}-AngIV. Hinge had previously validated as an HGF antagonist by its ability to inhibit HGF-dependent c-Met phosphorylation and HGF-dependent cellular responses including scattering of Madin-Darby canine kidney (MDCK) cells (Kawas *et al.*, 2011).

Hinge alone was found to have no effect on spinogenesis over a wide range of doses (10^{-8} M – 10^{-12} M) in dissociated hippocampal neurons, thus suggesting that Hinge and the HGF/c-Met system do not have a significant role in the basal spinogenesis seen in the cultured neurons. However, Hinge was effective at inhibiting spine formation in neurons stimulated with 10 ng/ml HGF (Figure 6A), 10^{-12} M Dihexa (Figure 6B), or 10^{-12} M Nle^{1}-AngIV (Figure 6C) further supporting the contention that these actions are mediated by the HGF/c-Met system.

To assess the effects of Hinge on glutamate inputs, mEPSCs were recorded from mRFP-β-actin transfected hippocampal neurons treated for 5 days with Hinge (10^{-12} M), HGF (10 ng/ml), Dihexa (10^{-12} M), Hinge + HGF (10^{-12} M + 10 ng/ml, respectively) or Hinge + Dihexa (10^{-12} M each) (Figure 6D and E). Hinge alone did not affect mEPSC frequency (mean frequency = 3.96 ± 0.29, n = 38 (Figure 6D), and 4.00 ± 0.37, n = 23 (Figure 6E) compared to vehicle treated neurons (mean frequency = 4.81± 0.32, n = 44 (Figure 6D), and 3.72 ± 0.28, n = 44 (Figure 6E)). HGF and Dihexa significantly increased mEPSC frequency compared to both Hinge and vehicle

JPET Fast Forward. Published on September 3, 2014 as DOI: 10.1124/jpet.114.218735
This article has not been copyedited and formatted. The final version may differ from this version.

treated neurons (mean frequency for HGF = 9.08 ± 0.28, n = 46 and for Dihexa = 7.93 ± 0.38, n = 31). These effects are significantly attenuated by stimulation in the presence of Hinge (mean frequencies for HGF + Hinge = 5.16 ± 0.27, n = 38 and Dihexa + Hinge = 5.55 ± 0.35, n = 29). Together these results indicate that newly generated spines form functional synapses, and that Hinge has no effect on mEPSC frequency alone, but blocks the effects of Dihexa and HGF indicating their dependence on a functional HGF/c-Met system.

To further confirm that the synaptogenic effects of Dihexa and Nle^{1}-AngIV are HGF/c-Met system-dependent a shRNA specific for c-Met was employed to reduce receptor expression. Dissociated hippocampal neurons were transfected with mRFP-β-actin and shMet RNA and receptor knock-down was allowed to proceed for 48 h prior to stimulating with HGF (10 ng/ml), Dihexa or Nle^{1}-AngIV (both at 10^{-12} M). Neurons transfected with mRFP-β-actin alone, serving as the control, were treated with HGF, Dihexa or Nle^{1}-AngIV. A significant increase in the number of spines compared to control treated neurons was observed (mean spine numbers per 50 μm dendrite length = 13.2 vs. HGF = 20.6; Dihexa = 21.8 and Nle^{1}-AngIV = 20.0; $p < 0.05$ by one-way ANOVA followed by Tukey post hoc test). The spine numbers in neurons transfected with mRFP-β-actin and the shMet, which were stimulated with 10 ng/ml HGF, 10^{-12} M Dihexa, or Nle^{1}-AngIV, did not differ from controls (mean spine numbers per 50 μm dendrite length = 13.5 vs. HGF = 12.4; Dihexa = 12.0 and Nle^{1}-AngIV = 12.1; $p > 0.05$ by one-way ANOVA followed by Tukey post hoc test) as shown in Figure 6H**.** Application of a scrambled RNA sequence, which was employed as the negative control, had no effect on basal or stimulated spinogenesis (Figure 6H).

Because of the purposely low transfection rate required to visualize individual dendrites direct assessment of c-Met levels in the mRFP-β-actin labeled neurons was not feasible.

JPET Fast Forward. Published on September 3, 2014 as DOI: 10.1124/jpet.114.218735
This article has not been copyedited and formatted. The final version may differ from this version.

Nevertheless, in an attempt to gauge the general effectiveness of the sh-RNA human embryonic kidney (HEK) cells were transfected with 6-Myc-tagged c-Met (0.1 µg) alone, with the shMet, or with a scrambled control RNA (Figure 6F and G).

Together these results demonstrate that the pro-spinogenic/synaptogenic effects of AngIV analogs are mediated by activation of the HGF/c-Met system.

- ***The HGF Antagonist, Hinge, Blocks the Ability of Dihexa to Restore Cognitive Function.***

Previous studies from our laboratory have demonstrated that oral delivery of Dihexa can normalize or improve spatial learning in scopolamine deficit and aged rat dementia models (McCoy *et al.,* 2013). These results combined with the above data indicating that Dihexa-mediated synaptogenesis is HGF/c-Met-dependent predicts that intracerebroventricularly (*icv*) delivered Hinge, and HGF antagonist, should be able to block the capacity of orally delivered Dihexa to reverse scopolamine-dependent spatial learning deficits in rats. To evaluate the validity of this hypothesis spatial learning was monitored using the Morris water maze task, a hippocampal-dependent spatial learning task requiring rats to locate a pedestal hidden beneath the surface of the water by orienting to extra-maze cues. The groups tested included a control in which artificial cerebrospinal fluid (aCSF) was delivered *icv* followed by oral saline; *icv* scopolamine (70 nmoles) followed by oral saline, which was expected to instigate a learning deficit; *icv* scopolamine followed by oral Dihexa (2 mg/kg),which was anticipated to reverse the expected scopolamine-dependent cognitive deficit; *icv* aCSF followed by oral Dihexa (2 mg/kg); *icv* Hinge (300 pmoles) followed by oral saline; and *icv* scopolamine + Hinge followed by Dihexa, which was expected to blunt Dihexa's ability to restore cognitive function. Figure 7C presents the mean latencies to find the hidden pedestal for days 1-8 of training in the water maze. None of the groups differed significantly in latency to find the pedestal on day one of training

JPET Fast Forward. Published on September 3, 2014 as DOI: 10.1124/jpet.114.218735
This article has not been copyedited and formatted. The final version may differ from this version.

with mean latencies for the vehicle control (aCSF → saline) group = 71.0 s; the scopolamine → saline group = 109.9 s; the aCSF→ Dihexa group = 117.5 s; the Hinge → saline group = 90.4 s; the scopolamine → Dihexa group = 115.2 s; and, the scopolamine + Hinge → Dihexa treated group = 107.9 s ($p > 0.05$). By the fourth day of training the scopolamine → saline group (mean latency to find the pedestal = 88.7 s) and the scopolamine + Hinge → Dihexa group (mean latency = 78.6 s) showed little sign of improvement compared to the aCSF control group (mean latency = 30.4 s), the Hinge → saline group (mean latency = 37.2 s) and the scopolamine → Dihexa group (mean latency = 35.5 s ($p < 0.05$), which were not different from one another ($p > .05$). On the final day of training when maximal learning had occurred the mean latencies for the scopolamine → saline group (mean latency to find the pedestal = 69.8 s) and the scopolamine + Hinge → Dihexa group (mean latency = 71.0 s), which were not different from one another ($p > 0.05$), indicated little improvement in learning compared to the aCSF control group (mean latency = 11.8 s); the Hinge → saline group (mean latency = 17.7 s); the aCSF → Dihexa group (mean latency = 25.4 s); and the scopolamine → Dihexa group (mean latency = 18.6 s). Together these data indicate that the improved cognitive function observed when Dihexa was delivered orally to scopolamine treated rats was the result of the activation of the central HGF/c-Met system.

JPET Fast Forward. Published on September 3, 2014 as DOI: 10.1124/jpet.114.218735
This article has not been copyedited and formatted. The final version may differ from this version.

DISCUSSION

The pro-cognitive effects of AngIV analogs have long been recognized and their potential as anti-dementia pharmaceuticals widely appreciated (Braszko *et al.*, 1988; Stubley-Weatherly, 1996; Pederson *et al.*, 1998; Wright *et al.*, 1999; Wright and Harding, 2011). Nevertheless, two obstacles have persistently impeded the development of clinically useful analogs: 1) poor pharmacokinetic properties; and, 2) the absence of an identified molecular target. The pharmacokinetic limitations of metabolic instability and an inability to pass the BBB have recently been overcome by the design and synthesis of Dihexa, a novel AngIV analog. Dihexa has documented pro-cognitive/ anti-dementia activity, is metabolically stable, BBB permeant, and orally active (McCoy *et al.*, 2013). Here we address the second issue that has been hindering the development of AngIV-based therapeutics, namely unknowns regarding the mechanism of action of AngIV analogs. Present results clearly demonstrate that the actions of AngIV analogs, including Dihexa, are dependent on activation of the HGF/c-Met system.

Initial hints regarding the equivalency of the AngIV/AT_4 and HGF/c-Met systems can be gleaned from an examination of their physiological signatures. Activation of the AngIV/AT_4 system is cerebroprotective (Date *et al.*, 2004; Faure *et al.*, 2006), augments long-term potentiation (Kramar *et al.*, 2001; Wayner *et al.*, 2001; Akimoto *et al.*, 2004; Davis *et al.*, 2006), induces dendritic and synaptic remodeling (Benoist *et al.*, 2011; McCoy *et al.*, 2013), stimulates hippocampal neurogenesis (Kawas and Harding unpublished), and has well established pro-cognitive effects (Wright and Harding 2011). Likewise, HGF displays profound neuroprotective activity (Doeppner *et al.*, 2011; Shang *et al.*, 2010), has a proven ability to potently stimulate both neurogenesis (Nicoleau *et al.*, 2009; Wang *et al.*, 2011; Shang *et al.*, 2011) and facilitates LTP (Akimoto *et al.*, 2004). HGF is a potent neurotrophic factor in many brain regions (Ebens

JPET Fast Forward. Published on September 3, 2014 as DOI: 10.1124/jpet.114.218735
This article has not been copyedited and formatted. The final version may differ from this version.

et al., 1996; Kato *et al.*, 2009), affecting a variety of neuronal cell types. Activation of the HGF/c-Met system has been shown to possess neuroprotective/neurorestorative activity related to amyotrophic lateral sclerosis (Kadoyama *et al.*, 2007), Parkinson's disease (Koike *et al.*, 2006; Lan *et al.*, 2008), spinal cord trauma (Kitamura *et al.*, 2011), and multiple sclerosis (Bai *et al.*, 2011). Moreover, activation of the HGF/c-Met system improves cognition (Akimoto *et al.*, 2004) – an outcome that may reflect its ability to induce dendritic remodeling (Tyndall and Walikonis, 2007) and spur neural stem cell proliferation and differentiation (Nicoleau *et al.*, 2009).

In addition to functional similarities there is sequence homology between AngIV, its analogs, and a small, 6-amino acid domain of HGF termed the "hinge" region, which participates in the process of HGF dimerization (Kawas *et al.*, 2012). Dimerization is required for HGF activation and ultimately the activation of its receptor, c-Met (Gherardi *et al.*, 2006; Youles *et al.*, 2008). Published studies with the AT_4 receptor antagonist, Norleual, illustrate its ability to bind to HGF with high affinity, compete for the binding of a "Hinge" peptide to HGF, and allosterically inhibit the ability of HGF to activate c-Met and induce cellular responses (Yamamoto *et al.*, 2010; Kawas *et al.*, 2011; Kawas *et al.*, 2012).

We hypothesize that AngIV analogs such as Nle^1-AngIV and Dihexa bind to and allosterically activate HGF better than HGF itself forming an active heterodimer of HGF:Dihexa. Further, we believe that HGF dimerization is a process designed to yield an active HGF conformation and not as typically suggested to mediate receptor dimerization. This supposition is based on our recent demonstration that, at least in rat hippocampal neurons, c-Met is pre-multimerized at postsynaptic densities as dimers, tetramers, hexamers, and octomers in the absence of HGF (Kawas *et al.*, 2013). Since the receptors are already assembled, an HGF-

JPET Fast Forward. Published on September 3, 2014 as DOI: 10.1124/jpet.114.218735
This article has not been copyedited and formatted. The final version may differ from this version.

mediated receptor dimerization process would be unnecessary and suggests that HGF dimerization may have another physiological role, namely to induce the active conformation of HGF. In concert with this hypothesis regarding Dihexa's positive allosterism we found that Dihexa bound to HGF with high affinity (Figure 1A) , disrupted HGF:HGF dimerization (Figure 1B), but resulted in a leftward shift of the HGF dose-response curve and augmentation of HGF's biological activity, even at sub-threshold concentrations of HGF (Figures 2 and 3).

If as hypothesized, the action of pro-cognitive AngIV analogs is mediated through activation of the HGF/c-Met system and since multiple AngIV analogs have previously been shown to stimulate dendritic spine growth in dissociated hippocampal neurons (Benoist *et al.*, 2011; McCoy *et al.*, 2013), we anticipated that HGF should exhibit similar activity. As predicted HGF promoted a dose-dependent increase in spinogenesis in dissociated hippocampal neurons that yielded functional synaptic connections (Figure 4A). The most effective concentration of HGF (10 ng/ml) was subsequently found to stimulate spinogenesis in hippocampal neurons in organotypic hippocampal slice cultures, which represent a more intact preparation (Figure 4B and C).

Most important to our hypothesis, the HGF antagonist, Hinge (Kawas *et al.*, 2011), inhibited the spinogenic activity of HGF, Nle^{1}-AngIV, and Dihexa (Figure 6A-C). Hinge, like Norleual, was established as a HGF antagonist based on its ability to bind HGF, inhibit HGF dimerization, block HGF-dependent c-Met phosphorylation and prevent HGF-dependent scattering in the MDCK epithelial cell line (Kawas *et al.*, 2012). In concert with these data transfection of rat hippocampal neurons with a c-Met sh-RNA similarly attenuated HGF-, Nle^{1}-AngIV-, and Dihexa-dependent spinogenesis (Figure 6F-H), thus substantiating the functional linkage between pro-cognitive AngIV analogs and the HGF/c-Met system. The concomitant ability of

JPET Fast Forward. Published on September 3, 2014 as DOI: 10.1124/jpet.114.218735
This article has not been copyedited and formatted. The final version may differ from this version.

Hinge to block HGF- and Dihexa-stimulated increase in mEPSC frequency in hippocampal neurons (Figure 6D and E) further indicates that Nle^1-AngIV- and Dihexa-dependent synaptogenesis is HGF dependent.

Despite Hinge's ability to block the capacity of HGF, Nle^1-AngIV, and Dihexa to induce spinogenesis and synaptogenesis, Hinge had no effect on basal spinogenesis or synaptogenesis in cultured hippocampal neurons suggesting that endogenous levels of HGF in the cultures were below the threshold concentration required for both processes (Figure 6D and H). Likewise, neither the HGF antagonist nor c-Met sh-RNA impacted basal levels of spinogenesis in the cultures. The observed capability of Nle^1-AngIV and Dihexa to induce spinogenesis and synaptogenesis in these same cultures offers additional support to the notion that both act by shifting HGF's dose-response curve to the left and render biologically sub-threshold levels of HGF physiologically meaningful.

Dihexa has recently been shown to augment the cognitive abilities of aged and scopolamine treated rats as assessed using the Morris water maze task (McCoy *et al.,* 2013). In order to expand our appraisal of the mechanism of action of pro-cognitive AngIV analogs to an *in vivo* setting we evaluated the ability of Hinge, to alter the pro-cognitive/anti-dementia action of Dihexa. Using an experimental paradigm identical to that employed in the McCoy (2013) study cognitive deficits were induced by *icv* application of the muscarinic receptor antagonist scopolamine, which renders rats acutely amnesic and therefore unable to learn the water maze task. As previously reported (McCoy *et al.,* 2013), orally delivered Dihexa reversed the cognitive deficits observed following scopolamine pretreatment. Most importantly *icv* co-application of Hinge with scopolamine blocked the capacity of Dihexa to rescue water maze performance. Application of Hinge alone had no impact on basal performance suggesting that

the HGF/c-Met system is not engaged during normal learning. This is consistent with previous Morris water maze results indicating that treatment with AngIV, or AngIV analogs, failed to facilitate learning and memory in normal functioning animals (Wright *et al.*, 1999). Alternatively, the consistent ability of an augmented HGF/c-Met system to support synaptic plasticity and to reverse nervous system deficits as documented here and by others suggests that the HGF/c-Met system is designed to respond to injury when markedly enhanced synaptic plasticity is beneficial as seen in stroke and neurodegenerative diseases. This notion is further supported by elevations in CNS HGF levels observed in several degenerative diseases (Shimamura *et al.*, 2007; Kato *et al.*, 2003; Salahi and Rajaei *et al.*, 2010; Muller *et al.*, 2012); perhaps representing the brain or spinal cord's attempt to activate regenerative processes

In summary, results presented here and elsewhere (Yamamoto *et al.*, 2010; Kawas *et al.*, 2011; Kawas *et al.*, 2012) support the hypothesis that the biological actions of AngIV analogs, including those that are pro-cognitive, are dependent upon interaction with HGF and subsequent modulation of c-Met activity. Furthermore these data are consistent with an allosteric model in which AngIV analogs bind to HGF inducing a conformational change. The presence of both high affinity HGF antagonists and activators that inhibit dimerization suggests that singlet HGF is capable of activating c-Met and that the function of dimerization is to support the active conformation of HGF. Ultimately, biophysical and structural studies will be needed to unequivocally confirm this allosteric model.

AUTHORSHIP CONTRIBUTIONS

Participated in research design: Benoist, Kawas, Harding, Wayman, Wright, Appleyard

Conducted experiments: Benoist, Kawas, Zhu, Wright, Stillmaker, Tyson

Contributed new reagents or analytical tools: Harding

Performed data analysis: Benoist, Kawas, Zhu, Harding, Wright, Tyson

Wrote or contributed to the writing of the manuscript: Harding, Benoist, Kawas, Zhu, Wright, Wayman, Appleyard

REFERENCES

Akimoto M, Baba A, Ikeda-Matsuo Y, Yamada MK, Itamura R, Nishiyama N, Ikegaya Y, Matsuki N. (2004) Hepatocyte growth factor as an enhancer of NMDA currents and synaptic plasticity in the hippocampus. Neuroscience 128: 155-162.

Albiston AL, Fernando RN, Yeatman HR, Burns P, Ng L, Daswani D, Diwakarla S, Pham V, Chai SY. (2010) Gene knockout of insulin-regulated aminopeptidase: loss of the specific binding site for angiotensin IV and age-related deficit in spatial memory. Neurobiol Learn Mem 93: 19-30.

Albiston AL, McDowall SG, Matsacos D, Sim P, Clune E, Mustafa T, Lee J, Mendelsohn FA, Simpson RJ, Connolly LM, Chai SY. (2001) Evidence that the angiotensin IV (AT(4)) receptor is the enzyme insulin-regulated aminopeptidase. J Biol Chem 276: 48623-48626.

Bai L, Lennon DP, Caplan AI, DeChant A, Hecker J, Kranso J, Zaremba A, Miller RH. (2012) Hepatocyte growth factor mediates mesenchymal stem cell-induced recovery in multiple sclerosis models. Nat Neurosci 15:862-870.

Balschun D, Moechars D, Callaerts-Vegh Z, Vermaercke B, Van Acker N, Andries L, D'Hooge R. (2010) Vesicular glutamate transporter VGLUT1 has a role in hippocampal long-term potentiation and spatial reversal learning. Cereb Cortex 20: 684-693.

Benoist CC, Wright JW, Zhu M, Appleyard SM, Wayman GA, Harding JW. (2011) Facilitation of hippocampal synaptogenesis and spatial memory by C-terminal truncated Nle1-angiotensin IV analogs. J Pharmacol Exp Ther 339: 35-44.

Braszko JJ, Kupryszewski G, Witczuk B, Wisniewski K. (1988) Angiotensin II-(3-8)-hexapeptide affects motor activity, performance of passive avoidance and a conditioned avoidance response in rats. Neuroscience 27: 777-783.

Chen JK, Zimpelmann J, Harris RC, Burns KD. (2001) Angiotensin IV induces tyrosine phosphorylation of focal adhesion kinase and paxillin in proximal tubule cells. Am J Physiol Renal Physiol 280: F980-F988.

Date I, Takagi N, Takagi K, Kago T, Matsumoto K, Nakamura T, Takeo S. (2004) Hepatocyte growth factor improved learning and memory dysfunction of microsphere-embolized rats. J Neurosci Res 78: 442-453.

Davis CJ, Kramar EA, De A, Meighan PC, Simasko SM, Wright JW, Harding JW. (2006) AT_4 receptor activation increases intracellular calcium influx and induces a non-N-methyl-D-aspartate dependent form of long-term potentiation. Neuroscience 137: 1369-1379.

Doeppner TR, Kaltwasser B, ElAli A, Zechariah A, Hermann DM, Bähr M. (2011) Acute hepatocyte growth factor treatment induces long-term neuroprotection and stroke recovery via mechanisms involving neural precursor cell proliferation and differentiation. J Cereb Blood Flow Metab 31: 1251-1262.

Ebens A, Brose K, Leonardo ED, Hanson MG Jr, Bladt F, Birchmeier C, Barres BA, Tessier-Lavigne M. (1996) Hepatocyte growth factor/scatter factor is an axonal chemoattractant and a neurotrophic factor for spinal motor neurons. Neuron 17:1157-1172.

Faure S, Chapot R, Tallet D, Javellaud J, Achard JM, Oudart N. (2006) Cerebroprotective effect of angiotensin IV in experimental ischemic stroke in the rat mediated by AT_4 receptors. J Physiol Pharmacol 57: 329-342.

Ferreira A, Rapoport M. (2002) The synapsins: beyond the regulation of neurotransmitter release. Cell Mol Life Sci 59: 589-595.

Finsterwald C, Martin JL. (2011) Cellular mechanisms underlying the regulation of dendritic development by hepatocyte growth factor. Eur J Neurosci 34: 1053-1061.

Gherardi E, Sandin S, Petoukhov MV, Finch J, Youles ME, Ofverstedt LG, Miguel RN, Blundell TL, Vande Woude GF, Skoglund U, Svergun DI. (2006) Structural basis of hepatocyte growth factor/scatter factor and MET signaling. Proc Natl Acad Sci U S A 103: 4046-4051.

Hamilton TA, Handa RK, Harding JW, Wright JW. (2001) A role for the angiotensin IV/AT_4 system in mediating natriuresis in the rat. Peptides 22: 935-944.

Handa RK. (2001) Characterization and signaling of the AT(4) receptor in human proximal tubule epithelial (HK-2) cells. J Am Soc Nephrol 12:440-449.

Kadoyama K, Funakoshi H, Ohya W, Nakamura T. (2007) Hepatocyte growth factor (HGF) attenuates gliosis and motoneuronal degeneration in the brainstem motor nuclei of a transgenic mouse model of ALS. Neurosci Res 59: 446-456.

Kato S, Funakoshi H, Nakamura T, Kato M, Nakano I, Hirano A, Ohama E. (2003) Expression of hepatocyte growth factor and c-Met in the anterior horn cells of the spinal cord in the patients with amyotrophic lateral sclerosis (ALS): immunohistochemical studies on sporadic ALS and familial ALS with superoxide dismutase 1 gene mutation. Acta Neuropathol 106: 112-120.

Kawas LH, Benoist CC, Harding JW, Wayman GA, Abu-Lail NI. (2013) Nanoscale mapping of the Met receptor on hippocampal neurons by AFM and confocal microscopy. Nanomedicine 9: 428-438.

Kawas LH, McCoy AT, Yamamoto BJ, Wright JW, Harding JW. (2012) Development of Angiotensin IV Analogs as Hepatocyte Growth Factor/Met Modifiers. J Pharmacol Exp Ther 340: 539-548.

Kawas LH, Yamamoto BJ, Wright JW, Harding JW. (2011) Mimics of the dimerization domain of hepatocyte growth factor exhibit anti-met and anti-cancer activity. J Pharmacol Exp Ther 339: 509-518.

Kitamura K, Fujiyoshi K, Yamane J, Toyota F, Hikishima K, Nomura T, Funakoshi H, Nakamura T, Aoki M, Toyama Y, Okano H, Nakamura M. (2011) Human hepatocyte growth factor promotes functional recovery in primates after spinal cord injury. PLoS One 6: e27706.

Koike H, Ishida A, Shimamura M, Mizuno S, Nakamura T, Ogihara T, Kaneda Y, Morishita R. (2006) Prevention of onset of Parkinson's disease by in vivo gene transfer of human hepatocyte growth factor in rodent model: a model of gene therapy for Parkinson's disease. Gene Therap 13: 1639-1644.

Kramár EA, Armstrong DL, Ikeda S, Wayner MJ, Harding JW, Wright JW. (2001) The effects of angiotensin IV analogs on long-term potentiation within the CA1 region of the hippocampus in vitro. Brain Res 897: 114-121.

Kramár EA, Harding JW, Wright JW. (1997) Angiotensin II- and IV-induced changes in cerebral blood flow. Roles of AT_1, AT_2, and AT_4 receptor subtypes. Regulatory Pep 68: 131-138.

Lan F, Xu J, Zhang X, Wong VW, Li X, Lu A, Lu W, Shen L, Li L. (2008) Hepatocyte growth factor promotes proliferation and migration in immortalized progenitor cells. Neuroreport 19: 765-769.

Li YD, Block ER, Patel JM. (2002) Activation of multiple signaling modules is critical in angiotensin IV-induced lung endothelial cell proliferation. Am J Physiol Lung Cell Mol Physiol 283: L707-L716.

McCoy AT, Benoist CC, Kawas LH, Bule J, Zhu M, Appleyard SM, Wayman GA, Wright JW, Harding JW. (2013) Evaluation of metabolically stabilized angiotensin IV analogs as procognitive/antidementia agents. J Pharmacol Exper Therap 344: 141-154.

Müller AM, Jun E, Conlon H, Sadiq SA. (2012) Cerebrospinal hepatocyte growth factor levels correlate negatively with disease activity in multiple sclerosis. J Neuroimmunol 15: 80-86.

Nicoleau C, Benzakour O, Agasse F, Thiriet N, Petit J, Prestoz L, Roger M, Jaber M, Coronas V. (2009) Endogenous hepatocyte growth factor is a niche signal for subventricular zone neural stem cell amplification and self-renewal. Stem Cells 27: 408-419.

Peters S, Adjei AA. (2012) MET: a promising anticancer therapeutic target. Nat Rev Clin Oncol 9: 314-326.

Pederson ES, Krishnan R, Harding JW, Wright JW. (2001) A role for the angiotensin AT_4 receptor subtype in overcoming scopolamine-induced spatial memory deficits. Reg Pep 102: 147-156.

Salehi Z, Rajaei F. (2010) Expression of hepatocyte growth factor in the serum and cerebrospinal fluid of patients with Parkinson's disease. J Clin Neurosci 17: 1553-1556.

Shang J, Deguchi K, Yamashita T, Ohta Y, Zhang H, Morimoto N, Liu N, Zhang X, Tian F, Matsuura T, Funakoshi H, Nakamura T, Abe K. (2010) Antiapoptotic and antiautophagic effects of glial cell line-derived neurotrophic factor and hepatocyte growth factor after transient middle cerebral artery occlusion in rats. J Neurosci Res 88: 2197-2206.

Shimamura M, Sato N, Sata M, Wakayama K, Ogihara T, Morishita R. (2007) Expression of hepatocyte growth factor and c-Met after spinal cord injury in rats. Brain Res 1151 :188-194.

Stella MC, Comoglio PM. (1999) HGF: a multifunctional growth factor controlling cell scattering. Int J Biochem Cell Biol 31: 1357-1362.

Stubley-Weatherly L, Harding JW, Wright JW. (1996) Effects of discrete kainic acid-induced hippocampal lesions on spatial and contextual learning and memory in rats. Brain Res 716: 29-38.

Swanson GN, Hanesworth JM, Sardinia MF, Coleman JK, Wright JW, Hall KL, Miller-Wing AV, Stobb JW, Cook VI, Harding EC. (1992) Discovery of a distinct binding site for angiotensin II (3-8), a putative angiotensin IV receptor. Reg Pep 13: 409-419.

Tyndall SJ, Patel SJ, Walikonis RS. (2007) Hepatocyte growth factor-induced enhancement of dendritic branching is blocked by inhibitors of N-methyl-D-aspartate receptors and calcium/calmodulin-dependent kinases. J Neurosci Res 85: 2343-2351.

Wang TW, Zhang H, Gyetko MR, Parent JM. (2011) Hepatocyte growth factor acts as a mitogen and chemoattractant for postnatal subventricular zone-olfactory bulb neurogenesis. Mol Cell Neurosci 48: 38-50.

Wayman GA, Davare M, Ando H, Fortin D, Varlamova O, Cheng HY, Marks D, Obrietan K, Soderling TR, Goodman RH, Impey S. (2008) An activity-regulated microRNA controls dendritic plasticity by down-regulating p250GAP. Proc Natl Acad Sci U S A 105: 9093-9098.

Wayman GA, Impey S, Marks D, Saneyoshi T, Grant WF, Derkach V, Soderling TR. (2006) Activity-dependent dendritic arborization mediated by CaM-kinase I activation and enhanced CREB-dependent transcription of Wnt-2. Neuron 50: 897-909.

Wayner MJ, Armstrong DL, Phelix CF, Wright JW, Harding JW. (2001) Angiotensin IV enhances LTP in rat dentate gyrus in vivo. Peptides 22: 1403-1414.

Wright JW, Harding JW. (2011) The brain RAS and Alzheimer's disease. Exp Neurol 223: 326-333.

Wright JW, Harding JW. (2013) The brain renin-angiotensin system: a diversity of functions and implications for CNS diseases. Pflugers Arch 465: 133-151.

Wright JW, Stubley L, Pederson ES, Kramár EA, Hanesworth JM, Harding JW. (1999) Contributions of the brain angiotensin IV-AT_4 receptor subtype system to spatial learning. J Neurosci 19: 3952-3961.

Yamamoto BJ, Elias PD, Masino JA, Hudson BD, McCoy AT, Anderson ZJ, Varnum MD, Sardinia MF, Wright JW, Harding JW. (2010) The angiotensin IV analog Nle-Tyr-Leu-Ψ-(CH2-NH2)3-4-His-Pro-Phe (Norleual) can act as a Hepatocyte Growth Factor/c-Met inhibitor. J Pharmacol Exp Ther 333: 161-173.

Youles M, Holmes O, Petoukhov MV, Nessen MA, Stivala S, Svergun DI, Gherardi E. (2008) Engineering the NK1 fragment of hepatocyte growth factor/scatter factor as a MET receptor antagonist. J Mol Biol 377: 616-622.

Zhang YW, Vande Woude GF. (2003) HGF/SF-met signaling in the control of branching morphogenesis and invasion. J Cell Biochem 88: 408-417.

FOOTNOTES

Funding for this project was provided by grants from the Michael J. Fox Foundation and M^3 Biotechnology, Inc. to J.W.H.; NIH grant MH086032 and a Hope for Depression Research Foundation grant to GAW; a grant from the Edward E. and Lucille I. Lainge Endowment for Alzheimer's Research to J.W.W.; and the state of Washington.

Conflict of Interest: Joseph W. Harding and John W. Wright are co-founders and major shareholders of M^3 Biotechnology, Inc., which is developing HGF mimetics and antagonists for the treatment of various disorders including dementia. Leen H. Kawas is also the CEO of M^3 Biotechnology, Inc.

* Caroline Benoist and Leen Kawas contributed equally to this project.

JPET Fast Forward. Published on September 3, 2014 as DOI: 10.1124/jpet.114.218735
This article has not been copyedited and formatted. The final version may differ from this version.

FIGURE LEGENDS

Figure 1. Binding of the HGF mimetic, Dihexa, to HGF and its impact on HGF dimerization. (A) Dihexa binds saturably and with high affinity to HGF. The binding of ^{3}H-Dihexa to HGF was assessed using a soluble binding assay. Saturation isotherms were developed for the interaction of ^{3}H-Dihexa with HGF. 250 µl of PBS containing human HGF (1.25 ng) were incubated with multiple concentrations of ^{3}H-Dihexa ranging from 10^{-13} M to 10^{-8} for 40 minutes at 37°C. The incubates were then spun through Bio-Gel P6 spin columns (400 µl packed volume) for 1 minute to separate free and bound ^{3}H-Dihexa and the eluent collected and counted. Graph is a composite of three experiments run in quadruplicate. N=3, Mean ± SEM. (Kd=6.52 x 10^{-11} M). **(B) Dihexa blocks HGF dimerization**. HGF dimerization was assessed in the presence of various analogs* including Dihexa. Norleual, the Nle-X-6AHA (Cys, Met, Trp) analogs, and HGF Hinge have been shown to be HGF antagonists (Yamamoto *et al.,* 2010; Kawas *et al.,* 2011; Kawas *et al.,* 2012). Dimerization was carried out for 30 minutes in the presence of heparin. Samples where cross-linked with BS3 and separated by native PAGE. Bands were visualized by silver staining and **(C)** quantitated by densitometry. N=6. *** p<.001. * Some of data in (B) was previously published (Kawas *et al.,* 2012) and is being presented for comparison purposes with the permission of the publisher.

Figure 2. The HGF mimetics, Dihexa and Nle^{1}-AngIV, allosterically regulate HGF resulting in c-Met activation. The effect of Dihexa and Nle^{1}-AngIV on HGF-dependent c-Met activation was assessed in HEK 293T cells and analyzed for phosphorylated (activated) and total c-Met by immunoblotting. **(A)** An SDS PAGE illustrates the impact of Dihexa at 10^{-10} M and 10^{-12} M on

JPET Fast Forward. Published on September 3, 2014 as DOI: 10.1124/jpet.114.218735
This article has not been copyedited and formatted. The final version may differ from this version.

HGF-dependent c-Met phosphorylation. **(B)** Dihexa at 10^{-10} M augmented the effect of HGF at 1.25 ng/ml ($p<0.001$) and 2.5 ng/ml ($p<0.001$). Similarly Dihexa at 10^{-12} M augmented HGF's activity at 1.25 ng/ml ($p<0.001$) and 2.5 ng/ml ($p<0.001$). Neither Dihexa at 10^{-10} M nor at 10^{-12} M stimulated c-Met phosphorylation beyond background. No significant change in total c-Met was observed in any experimental group. N=4; Mean ± SEM. **(C)** An SDS PAGE illustrates the impact of Nle^1-AngIV at 10^{-10} M and 10^{-12} M on HGF-dependent c-Met phosphorylation. **(D)** Nle^1-AngIV at 10^{-10} M (***$p<0.001$) and 10^{-12} M (**$p<0.01$) augmented the effect of HGF at 1.25 ng/ml and Nle^1-AngIV at 10^{-10} M and 10^{-12} M augmented HGF's activity at 2.5 ng/ml (***$p<0.001$). Nle^1-AngIV alone at 10^{-10} M stimulated c-Met phosphorylation beyond background ($p<0.05$). No significant change in total c-Met was observed in any experimental group. N=4; Mean ± SEM. Together these data demonstrate the capacity of HGF mimetics to shift the dose-response curve of HGFs activation of c-Met to the left.

Figure 3. Effect of the HGF mimetics, Dihexa and Nle^1-AngIV, HGF-dependent cell scattering. Cell scattering was assessed in MDCK cells. Cells were grown to confluence on coverslips, which were then transferred to a clean plate. HGF, Dihexa, or Nle^1-AngIV alone or in combination was then added to the media at various concentrations. After treatment for four days, the number of cells that had scattered off the coverslip was quantitated. **(A)** HGF at 5 ng/ml significantly stimulated cell scattering ($p<0.001$). The addition of Dihexa at 10^{-10} M further increased scattering (**$p<0.01$). Dihexa alone at 10^{-12} M was able to enhance scattering ($p<0.01$). Examples of the effect of Dihexa are illustrated in **(B)**. Nle^1-AngIV at 10^{-8} M, 10^{-10} M,

JPET Fast Forward. Published on September 3, 2014 as DOI: 10.1124/jpet.114.218735
This article has not been copyedited and formatted. The final version may differ from this version.

and 10^{-12} M stimulated cell scattering (# and **p<0.05-0.01). Nle^1-AngIV at 10^{-14} M had no effect on scattering **(C)**. Examples of the effect of Dihexa are illustrated in **(D)**.

Figure 4. (A) HGF dose-dependently enhances spinogenesis. Dissociated hippocampal neurons from 1 or 2 day old rats were transfected with mRFP-β-actin and stimulated with HGF for 5 days. Treatment with 2.5 ng/ml of HGF did not affect basal spine numbers and was considered sub-threshold. Doses of 5, 10 and 20 ng/ml significantly increased the number of spines per 50 μm dendrite lengths compared to vehicle control treated neurons. *** p<0.001; **p<.01; Mean ± SEM.; N = 50 per treatment group. **(B & C) Effects of Dihexa and HGF on spinogenesis in organotypic hippocampal slice cultures.** Hippocampal slice cultures were biolistically transfected with the red soluble protein Tomato on DIV3 and stimulated with Dihexa or HGF on DIV5. **(B)** Representative images of CA1 neurons from slices that were either treated with vehicle (control), 10^{-12} M Dihexa or 10 ng/ml HGF for 2 days. **(C)** Bar graph showing quantitated spine density per 50 μm of dendrite length for each treatment group. Dihexa and HGF significantly increased the number of spines on CA1 hippocampal neurons compared to control treated (Mean ± SEM; N=50; ***p<0.001). **(D & E) Effects of combined sub-threshold doses of Nle^1-AngIV, Dihexa, and HGF on spinogenesis. (D)** Sub-threshold levels of HGF 2.5 ng/ml) and Nle^1-AngIV (10^{-13} M) did not affect basal spine numbers. However the combination of sub-threshold Nle^1-AngIV (10^{-13} M) and HGF (2.5 ng/ml) produced a significant induction of spinogenesis (***p<0.001) that was equivalent to that seen with supra-threshold HGF (10 ng/ml) or Nle^1-AngIV (10^{-12} M). **(E)** Sub-threshold levels of HGF (2.5 ng/ml) and Dihexa (10^{-13} M) did not affect basal spine numbers. However the combination of sub-

JPET Fast Forward. Published on September 3, 2014 as DOI: 10.1124/jpet.114.218735
This article has not been copyedited and formatted. The final version may differ from this version.

threshold Dihexa (10^{-13} M) and HGF (2.5 ng/ml) produced a significant induction of spinogenesis (***$p<0.001$) that was equivalent to that seen with supra-threshold HGF (10ng/ml) or Dihexa (10^{-12} M). The ability of combined agonists at sub-threshold doses to generate maximal responses suggests a commonality of receptor pathways. Mean ± SEM.; n=50.

Figure 5. Effect of HGF treatment on synaptogenesis in dissociated hippocampal neurons. HGF treatment supports the formation of functional synapses as indicated by a high correlation between postsynaptic spines (red) and markers of presynaptic active zones (green). **(A)** Representative images of hippocampal neurons transfected with mRFP-β-actin on DIV6 and treated with 10 ng/ml of HGF or vehicle for 5 days. The neurons were stained for the general presynaptic marker synapsin and the glutamatergic presynaptic marker VGLUT1. **(B)** Bar graph demonstrating an active phenotype as indicated by a significant increase in the number of spines per 50 µm of dendrite length following stimulation with HGF (10 ng/ml). Mean number of spines, HGF=33 vs. control=23; Mean ± SEM; N=25; ***$p<0.001$. **(C)** Percent correlation of actin-enriched postsynaptic spines (red) juxtaposed to the universal presynaptic marker synapsin (green). NS= $p>0.05$. The high percent correlation suggests functional synapses are formed. (**D)** Percent correlation of actin-enriched spines (red) juxtaposed to the glutamatergic presynaptic marker VGLUT1 (green). NS= $p>0.05$. A greater than 95% correlation suggests many of these inputs are glutamatergic. **(E)** Effect of Dihexa and HGF treatment on the frequency of mEPSCs in dissociated hippocampal neurons. Dissociated hippocampal neurons transfected with mRFP-β-actin were stimulated with 10^{-12} M Dihexa or 10 ng/ml for 5 days prior to recording mEPSCs. Neurons were treated with tetrodotoxin, picrotoxin, and strychnine to block sodium channels,

$GABA_A$, and glycine receptors. Treatment with both agonists significantly enhanced AMPA-receptor mediated currents compared to vehicle treated neurons Mean ± SEM; n = 9 respectively; ***p<0.012 HGF vs. Control; P <0.04 Hex vs. Control).

Figure 6. Effects of the HGF antagonist, Hinge, and a Met shRNA on spinogenesis. Dissociated hippocampal neurons from 1 or 2 day old rats were transfected with mRFP-β-actin and stimulated with HGF, Dihexa, or Nle^1-AngIV ± the HGF antagonist Hinge for 5 days (Kawas *et al.*, 2011). Mean ± SEM; N=50). **(A)** As has been seen previously, HGF induced spine formation (***p<0.001) while application with Hinge, had no impact on spine formation. Co-application Hinge with HGF, however, completely suppressed spine induction (###p<0.001). **(B)** Dihexa similarly induced spine formation (***p<0.001) and co-application with Hinge reversed the effect (###p<0.001). **(C)** Likewise, Nle^1-AngIV induced spine formation (***p<0.001) and co-application with Hinge reversed the effect (###p<0.001). In order to confirm that blockade of HGF's effect on spinogenesis by Hinge translated to a reduction in the frequency of mini-excitatory post-synaptic currents (mEPSCs), voltage clamp recordings were made from dissociated hippocampal neurons were following 5 days of treatment with drug. **(D)** As had been observed previously, HGF treatment increased the frequency of mEPSCs (***p<0.001) while Hinge had no effect on basal frequencies. However, co-application of Hinge with HGF suppressed the observed increase in frequencies (#p<0.028) (Mean ± SEM; N=38-46). **(E)** Dihexa treatment was again found to increase the frequency of mEPSCs (***p<0.001) Similar to what was observed with the HGF treatment, co-application of Hinge blocked the Dihexa-dependent increase in frequency (#p<0.01) (Mean ± SEM; N=23-44). A shRNA targeting c-Met

JPET Fast Forward. Published on September 3, 2014 as DOI: 10.1124/jpet.114.218735
This article has not been copyedited and formatted. The final version may differ from this version.

was designed using the RNAi central design program and inserted into the pSUPER vector under the control of the H1 promoter. In order to validate the effectiveness of the shMet HEK293T cells were co-transfected with the shMet vector and c-Met-6-Myc tagged pCAGGS-6-Myc destination vector. **(F)** As can be seen in the representative gel, the c-Met-6-Myc construct was effectively expressed compared to no-transfected controls **(G**; ***$p<0.001$; Mean ± SEM; N=4**)**. C-Met-6-Myc expression was significantly suppressed by co-transfection of the shMet vector (***$p<0.001$) but not by a co-transfected scrambled oligo-containing vector ($p>0.05$). **(H)** After validating the effectiveness of the shMet construct, dissociated hippocampal neurons from 1 or 2 day old rats were transfected with mRFP-β-actin and treated with HGF, Dihexa, or Nle^1-AngIV for 5 days. Some groups were co-transfected with either shMet or a scrambled control vector. HGF, Dihexa, and Nle^1-AngIV all induced spine formation ($p<0.001$), while shMet completely blocked spine induction by all three agonists (**$p<0.01$) the scrambled construct had no effect (#$p>0.05$) (Mean ± SEM; N=50).

Figure 7. Effect of The HGF antagonist, Hinge, on Dihexa's ability to restore spatial learning in the scopolamine amnesia model. Twenty minutes before beginning daily testing 3 month old male Sprague Dawley rats were given scopolamine (70 nmoles) or an artificial cerebrospinal fluid (aCSF) vehicle intracerebroventricularly followed immediately by oral delivery of Dihexa (2 mg/kg) or isotonic saline. When employed, Hinge (300 pmoles) in aCSF was delivered *icv* 5 minutes prior to testing. There were 5 trials per day for 8 days. The latency to find the pedestal was considered a measure of learning and memory. By day 7 oral (2 mg/kg) Dihexa was able to reverse the deficit seen with scopolamine and the performance was no

different than controls (*$p<0.05$). Similarly the aCSF/Dihexa and Hinge/saline groups were not different from the control and scopolamine/Dihexa groups ($p>0.05$). By day 7 all four of these groups were different from the scopolamine-Hinge/Dihexa and the scopolamine/saline groups. (Mean ± SEM; N=8-10). These data further indicate that oral Dihexa enters the brain and that its effects are mediated by the central HGF/c-Met system.

JPET Fast Forward. Published on September 3, 2014 as DOI: 10.1124/jpet.114.218735
This article has not been copyedited and formatted. The final version may differ from this version.

.

FIGURE 1

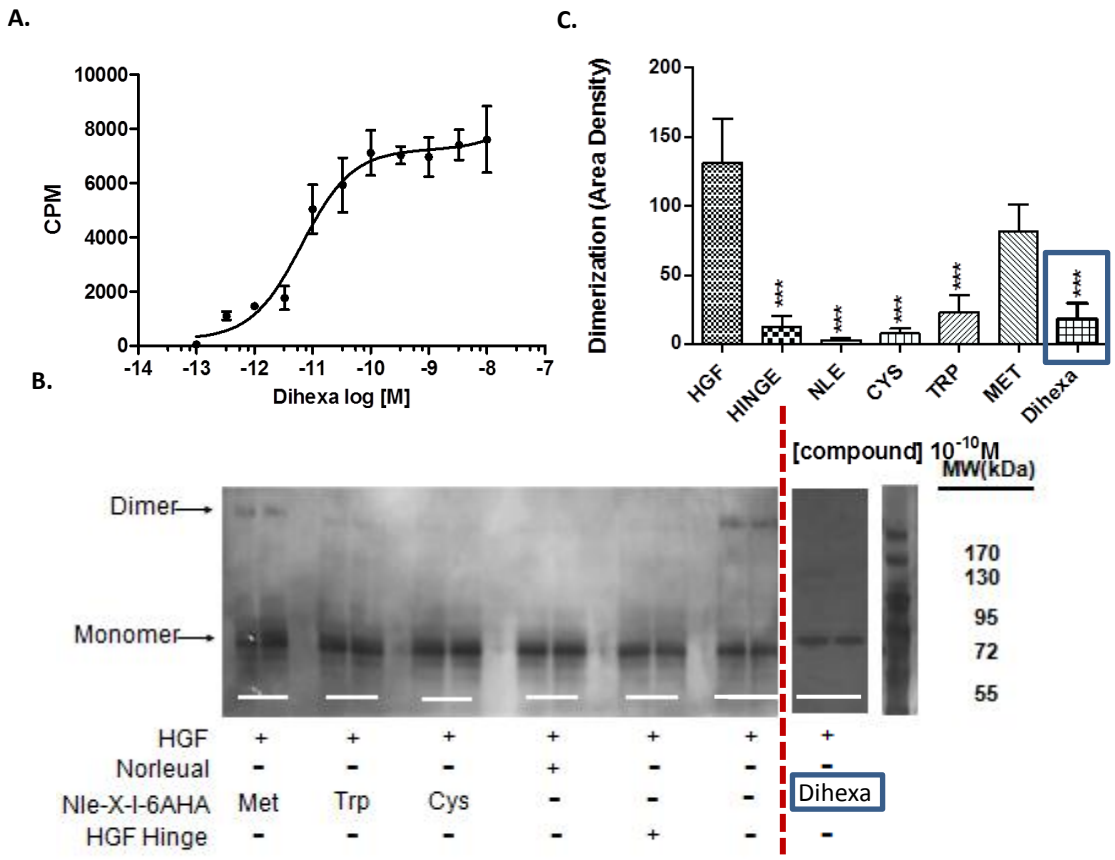

JPET Fast Forward. Published on September 3, 2014 as DOI: 10.1124/jpet.114.218735
This article has not been copyedited and formatted. The final version may differ from this version.

FIGURE 2

A.

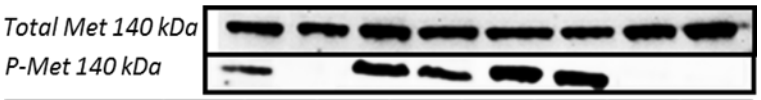

HGF 2.5 ng/ml	+	-	-	-	+	+	-	-
HGF 1.25 ng/ml	-	+	+	+	-	-	-	-
Dihexa 10^{-10} M	-	-	+	-	+	-	+	-
Dihexa 10^{-12} M	-	-	-	+	-	+	-	+

B.

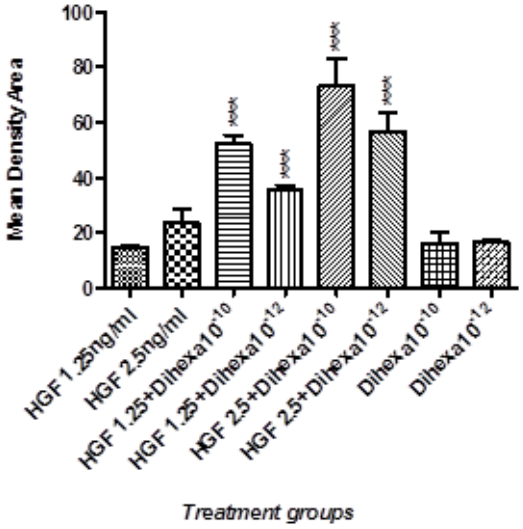

C.

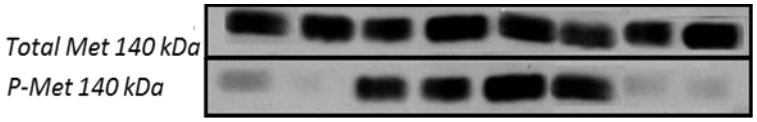

HGF 2.5 ng/ml	+	-	-	-	+	+	-	-
HGF 1.25 ng/ml	-	+	+	+	-	-	-	-
Nle¹ -AngIV 10^{-10} M	-	-	+	-	+	-	+	-
Nle¹ -AngIV 10^{-12} M	-	-	-	+	-	+	-	+

D.

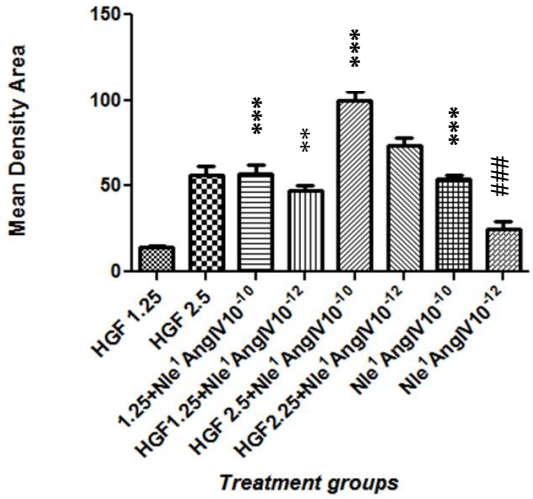

JPET Fast Forward. Published on September 3, 2014 as DOI: 10.1124/jpet.114.218735
This article has not been copyedited and formatted. The final version may differ from this version.

FIGURE 3

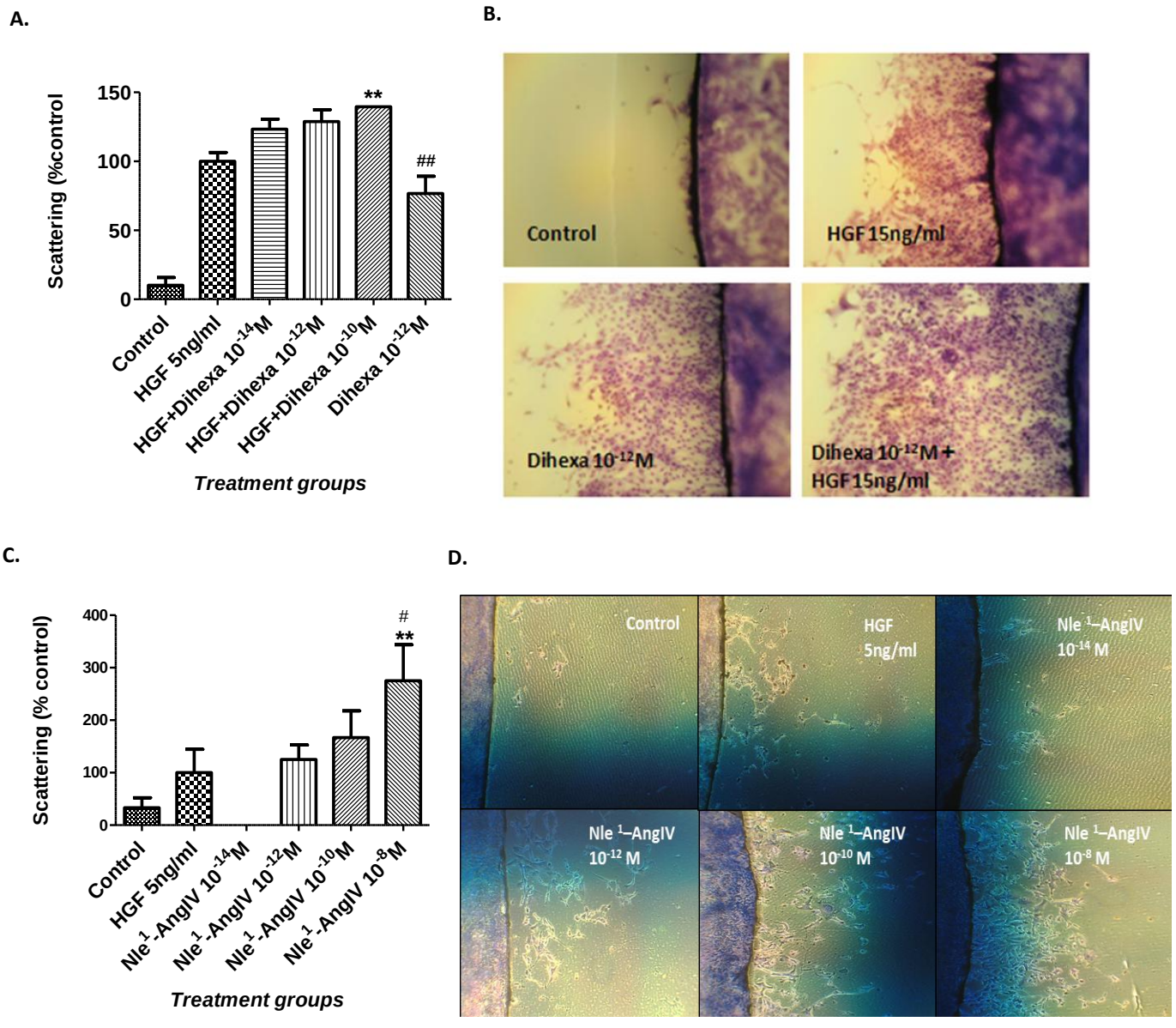

JPET Fast Forward. Published on September 3, 2014 as DOI: 10.1124/jpet.114.218735
This article has not been copyedited and formatted. The final version may differ from this version.

FIGURE 4

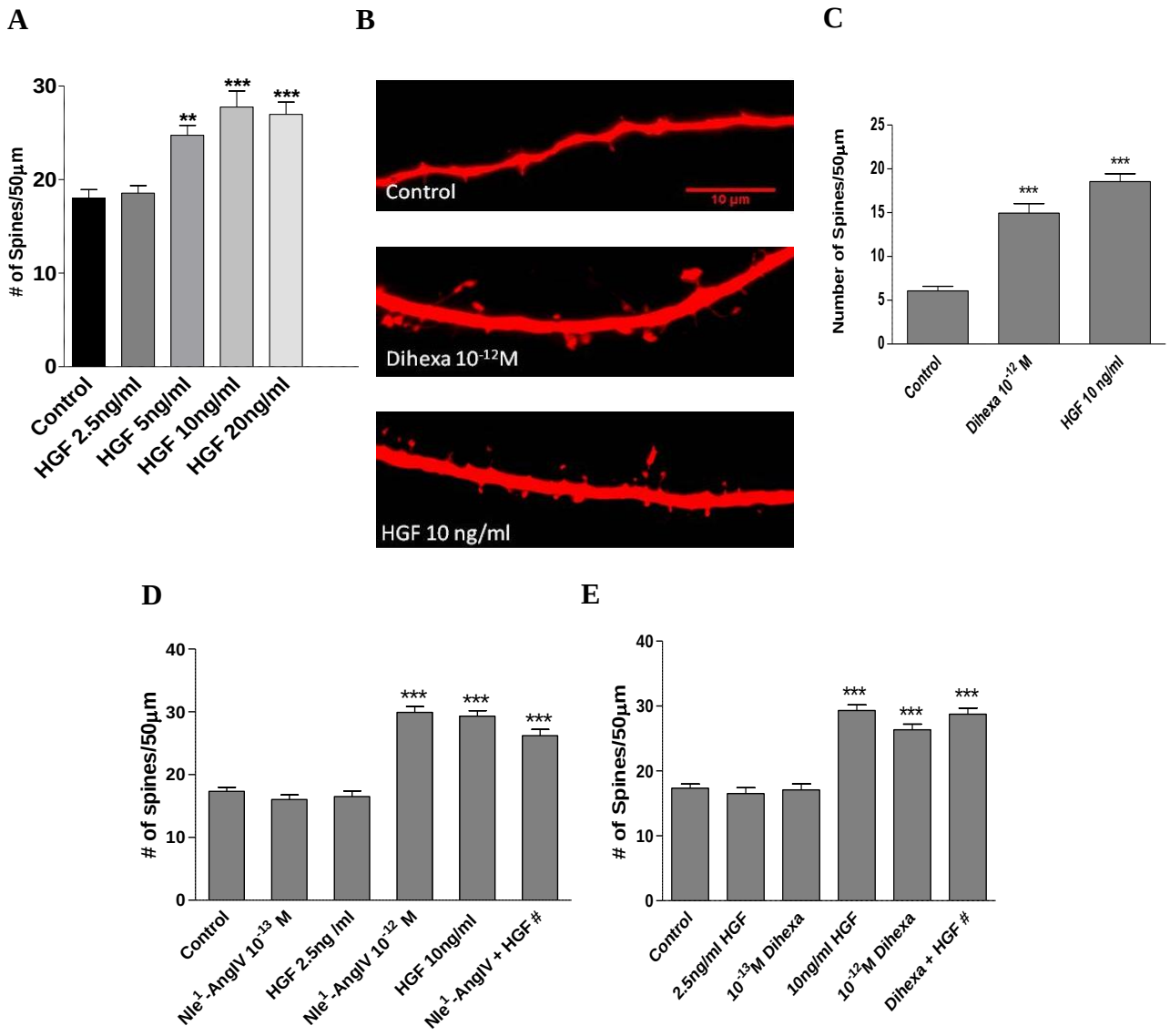

JPET Fast Forward. Published on September 3, 2014 as DOI: 10.1124/jpet.114.218735
This article has not been copyedited and formatted. The final version may differ from this version.

FIGURE 5

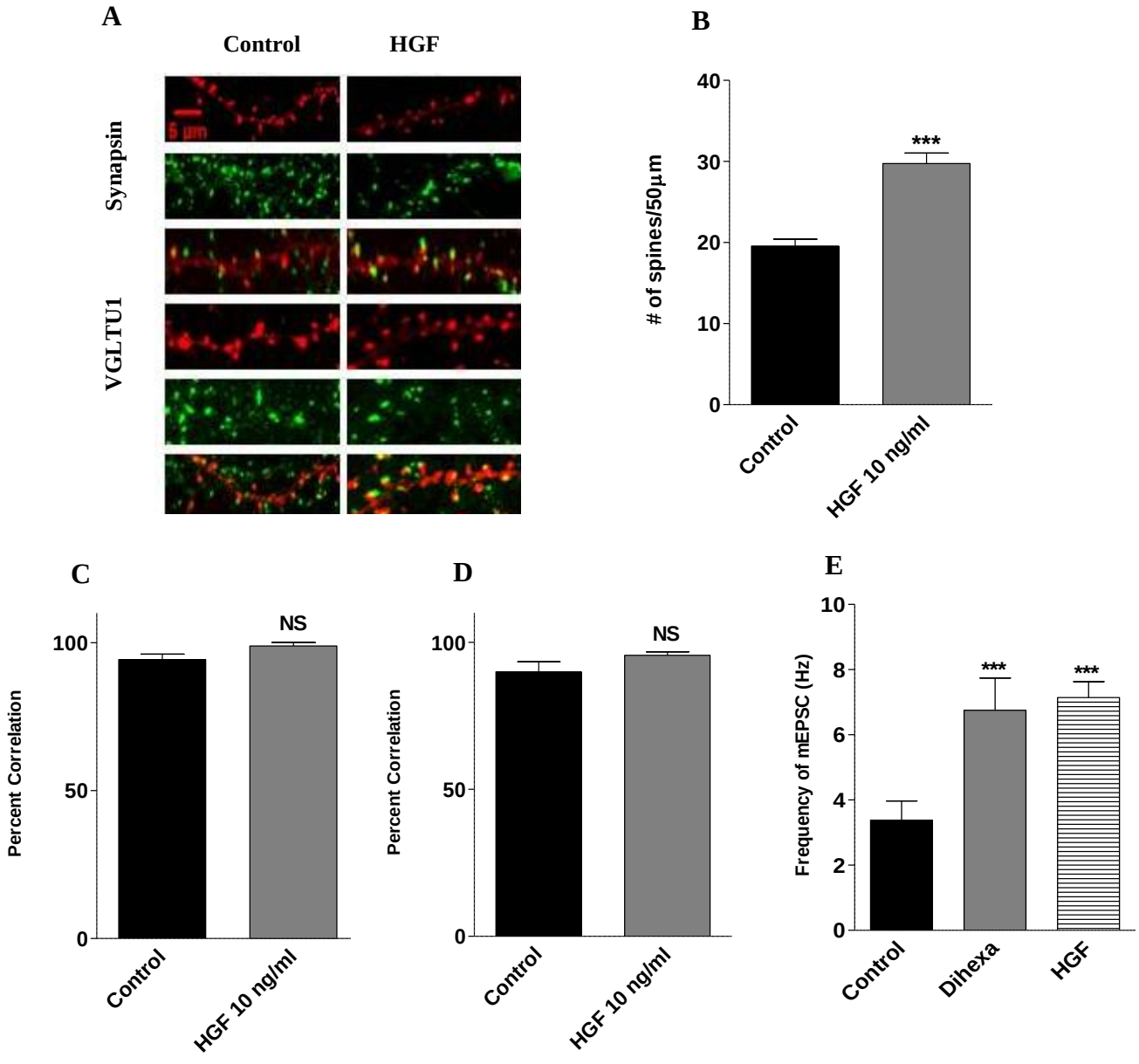

JPET Fast Forward. Published on September 3, 2014 as DOI: 10.1124/jpet.114.218735
This article has not been copyedited and formatted. The final version may differ from this version.

FIGURE 6

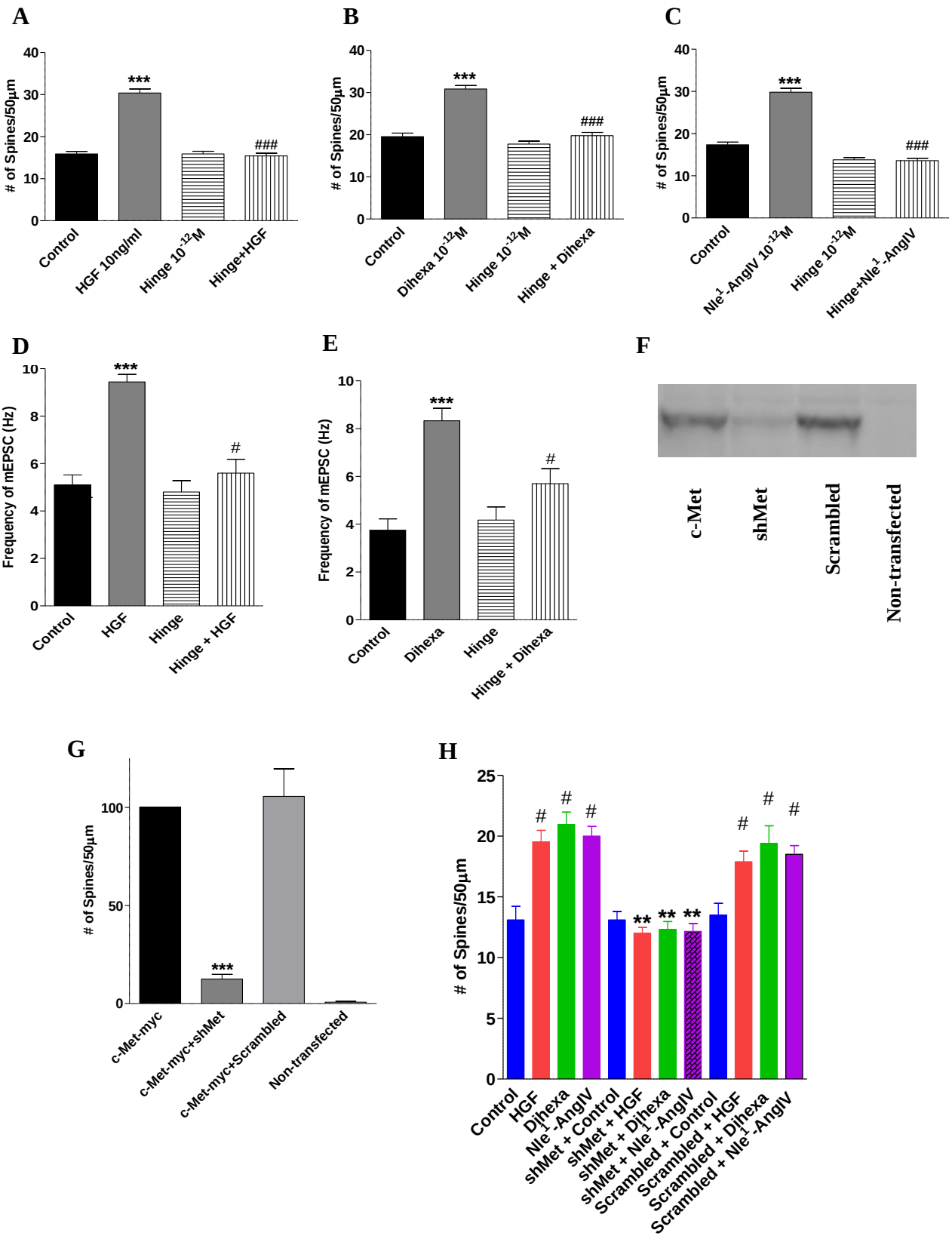

JPET Fast Forward. Published on September 3, 2014 as DOI: 10.1124/jpet.114.218735
This article has not been copyedited and formatted. The final version may differ from this version.

FIGURE 7